

Evaluating the Efficiency of Subsurface Drainages for Li-Shan Landslide in Taiwan

Der-Guey Lin¹, Sheng-Hsiung Hung², Cheng-Yu Ku³, Hsun-Chuan Chan^{4*}

¹Professor, Department of Soil and Water Conservation, National Chung-Hsing University

²Doctoral student, Department of Soil and Water Conservation, National Chung-Hsing University

³Professor, Department of Harbor and River Engineering, National Taiwan Ocean University

⁴Associate Professor, Department of Soil and Water Conservation, National Chung-Hsing University

hcchan@nchu.edu.tw (*corresponding authorsd: No. 250 Kuo-Kuang Road, Taichung 402, Taiwan)

Abstract: This study investigates the efficiency of subsurface drainage systems includes drainage wells (vertical shaft with drainage boreholes or horizontal drains) and drainage galleries (longitudinal tunnel with sub-vertical drainage boreholes) for the slope stabilization of Li-Shan landslide in central Taiwan. The efficiency of the subsurface drainages is verified through a series of two-dimensional (2-D) rainfall induced seepage and slope stability analyses without and with subsurface drainages remediation during two typhoon events. Numerical results and monitoring data both show that the groundwater level at B5 monitoring station with subsurface drainages remediation during Toraji Typhoon (2001) is about 40 m lower than that without remediation during Amber Typhoon (1997), and the factor of safety F_s of the first potential sliding surface (1^{st} -PSS, the most critical potential sliding surface) is promoted simultaneously from 1.096 to 1.228 due to the function of subsurface drainage systems. In addition, the F_s values of the three potential sliding surfaces (1^{st} -PSS, 2^{nd} -PSS, and 3^{rd} -PSS) stabilized by subsurface drainage systems are constantly maintained greater than unity ($F_s > 1.0$ or $F_s \geq 1.217$) during rainfalls with return periods increases from 25 to 50 and 100 years. This demonstrates the subsurface drainage systems in Li-Shan landslide are functional and capable of accelerating the drainage of infiltration rainwater induced from high intensity and long duration rainfall and protect the slope of landslide from further deterioration. This study provides a quick computation method to evaluate the effectiveness and efficiency of a subsurface drainage system with relatively high engineering costs for a large landslide.

Keywords: landslides, subsurface drainage systems, drainage boreholes, drainage well, drainage gallery, potential sliding surface, factor of safety

1. Introduction

The Li-Shan landslide has a long history of intermittent large movements toward down slope during rainfall since 1990 and currently has been stabilized by the subsurface drainage systems implemented by Taiwan government for seven years' duration from 1995 to 2002. The main remediation work for Li-Shan landslide was to lower the groundwater level through different subsurface drainage systems consisted of drain wells and drainage galleries. For subsurface drainage system, the effectiveness of horizontal drains on lowering the groundwater level and improving the slope stability is mainly governed by drain length, spacing, number, and installation location (Kenney et al., 1977; Prellwitz, 1978; Nonveiller, 1981; Lau and Kenney, 1984; Nakamura, 1988).

The function of horizontal drains has also been investigated by several numerical analyses. Cai et al. (1998) concluded that lengthening the horizontal drains is more effective than shortening the spacing and increasing the number of the horizontal drains in a group. Rahardjo et al. (2002, 2003, 2012) found that horizontal drains have little role in minimizing infiltration in an unsaturated residual soil slope and benefits of using horizontal drains can be obtained through the lowering of the groundwater table. In addition, the general trends of numerical results indicate the most benefit was derived from the drain located at the bottom of the slope. However, in the above analyses, the depth of horizontal drains is in comparatively shallow and unlike the deep drainage of Li-Shan landslide achieved by a series of drainage wells and drainage galleries. In addition, numerical modeling results, based on hydro-mechanically coupled 2-D distinct-element models, strongly suggest that deep drainage (drainage tunnel) was the key measure to successfully stabilize large landslides (Eberhardt et al., 2007).

Further, the potential effect of sub-vertical drains drilled from gallery (drainage gallery) on the stabilization of unstable slopes has been studied in large landslides using three-dimensional (3-D) numerical model considering hydro-geological and geo-mechanical parameter heterogeneity (Tacher et al., 2005; Matti, et. al, 2012). Although the 3-D modeling has a significant contribution on the reliability of ground movement computation, it requires a 3-D structural geological model and sophisticated transient hydro-geological model built by all available data includes boreholes, geophysics and field observations.

The efficiency of subsurface drainage systems constructed in Li-Shan landslide with relatively high construction costs (0.915 billion NT\$) has not yet been evaluated during torrential rainfall. In particular, the effects of the two drainage galleries ($G1$ - and $G2$ -gallery) on the slope stability of Li-Shan landslide during rainfall (or specific crisis) have not been inspected up-to-date. Using monitoring data and numerical techniques, this study aims at proposing a fast 2-D computation method to quantify the efficiency of subsurface drainages on the landslide stabilization considering the rainwater infiltration and transient water flow through unsaturated/saturated soils.

1.1 Location of Li-Shan Landslide Area

Li-Shan landslide is situated in Central Mountains at the northeast of Taichung City with a distance about 100 km and also at the intersection of Route Tai-8 and Route Tai-7 of the East-West cross-island highways where locates the landmark architecture Li-Shan Hotel as shown in Fig. 1.



Fig. 1 Overlook Li-Shan landslide area northward from Fu-Shou-Shan Farm at the upslope

61
62
63
64
65
66
67
68
69
70
71
72
73
74
75
76
77
78
79
80
81
82
83
84
85
86

1.2 Climate, Topography and Geology

The temperature in Li-Shan varies greatly between the day and the night and the temperature is about 15.2 °C on an average. In Li-Shan the average annual rainfall approximates 2,242 mm for an average annual rainy day of 176 days based on the rainfall records from 1978 to 2008. Annually, most of rainfall concentrates on Summer (from March to September) and the average monthly rainfall can reach 514 mm in May and June. In addition, the torrential rainfall occurred 7 or 8 times annually with rainfall intensity of 100 mm/day during June and September.

As shown in Fig. 2, the Li-Shan landslide situates at the west of Central Mountains with an area of around 230 hectares. The terrain of the landslide is descending from south to north with elevation varying from 2,100 to 1,800 m. The landslide is characterized by hilly and valley topography and the Da-Jai River flow from east to west through the northern edge of the landslide. The Li-Shan fault, a major ridge fault of Taiwan Island generated by the tectonic activity of the westward thrust front due to the collision between the Philippine Sea Plate and the Eurasian Plate, just locates at few kilometers west of the Li-Shan landslide. The geology of the landslide is categorized into Miocene Lu-Shan formation, highly fragmentary tertiary sub-metamorphic rock, and thick colluvium encountered locally and occasionally mixed with mudstone enriched with cleavage. Through the field data of boring log and geophysical exploration, the soil strata can be classified into five types from shallows to depths based on their weathering degree as shown in Fig. 3(a), namely, (1) colluvium, (2) heavily-weathered slate, (3) medium-weathered slate, (4) lightly-weathered slate, and (5) fresh slate. The material features of the five types were also evaluated by the *ISRM* classification as listed in Table 1 and it can be verified that the maximum weathering depth approximates 63 m at least. The landslide area can be divided into three regions, i.e. the west, northeast, and southeast regions. Except the southeast region, most of the unstable slopes possess shallow sliding planes about 9~26 m below ground surface. However, there is an old landslide within the southeast region. According to the core logs and the records of drainage gallery construction, the old sliding surface is located more than 40~60 m below ground surface.

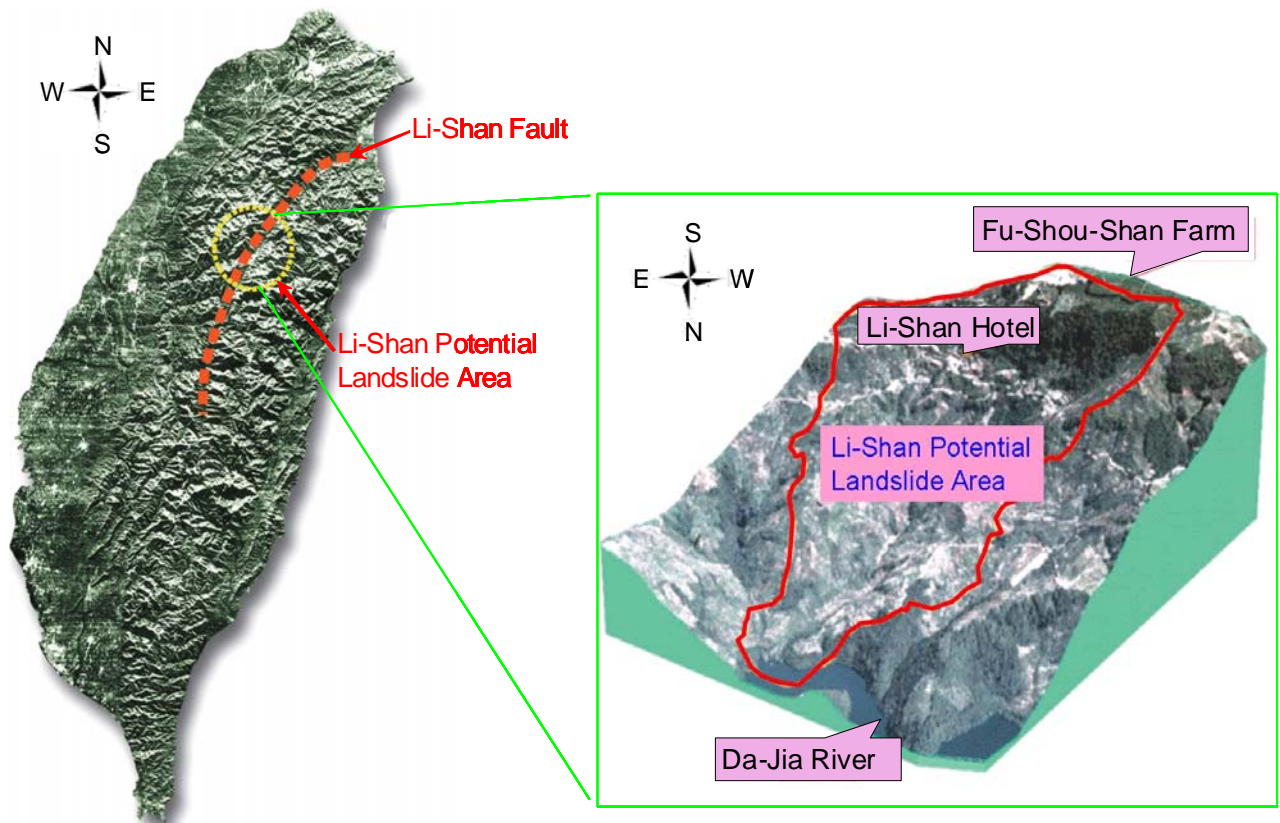


Fig. 2 Topographic and geological characteristics of Li-Shan landslide located at central Taiwan

87
88
89
90
91
92
93
94
95
96
97

Conclusively, the potential sliding surfaces are basically along the lower boundary of the regolith. The slide is mainly made up of the colluviums and heavily-weathered slate and forming the main part of the Li-Shan landslide. The outcrops of the Li-Shan landslide can be categorized into Miocene Lu-Shan formation and mainly consist of slate with color varied from black to deep gray as shown in Fig. 3(b). Nevertheless, the sliding bodies overlying the potential sliding surfaces of the landslide primarily is composed of weathered slate, fragment of slate and intercalary clayey strata. The properties of the sliding bodies exhibit a loose texture and poor grain size distribution which alternately leads to a less cementation, low strength, and high permeability geo-material. The composition of fresh slate can be visualized by microscopic image as displayed in Fig. 3(c).

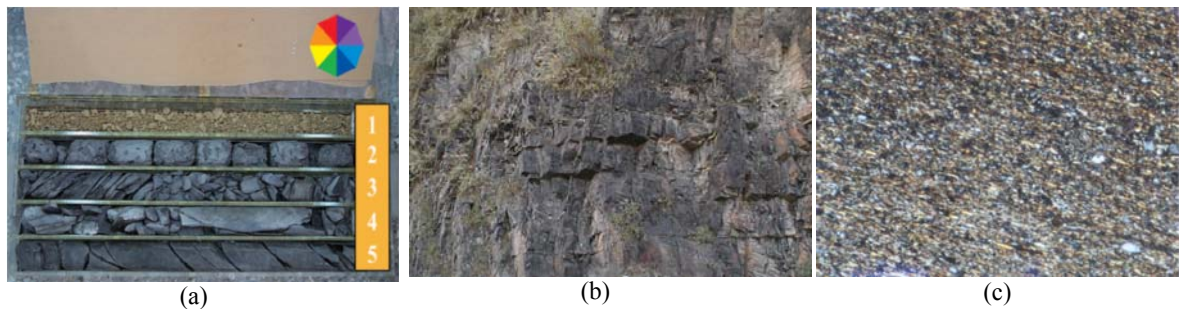


Fig. 3 (a) material types of soil strata (b) outcrops of slate formation (c) microscopic image of fresh slate of Li-Shan landslide

98
99

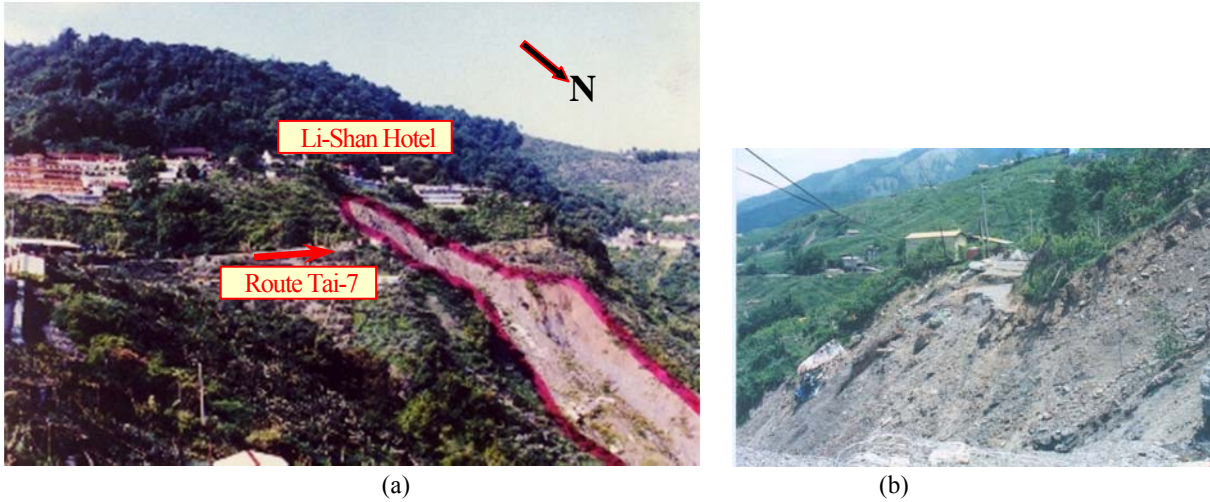
Table 1 Features of soil strata for Li-Shan landslide

Material (sampling depth: m)	Descriptions	ISRM
1. Colluvium (-1 m)	Sandy silt of yellowish-brown color mixed with rock fragments and gravel	VI
2. Heavily-weathered slate (-13 m)	Clayey soil, silty sand or sandy soil of black color with texture similar to fresh rock	V
3. Medium-weathered slate (-23 m)	Fragmentary rock core with thin sheet, black color, grain size of 2~30 mm and the outcrop enriched with fissure.	III, IV
4. Lightly-weathered slate (-18 m)	Blocky rock core with rounded shape, black color, grain size of 5~10 mm and the outcrop similar to fresh rock	II
5. Fresh slate (-63 m)	Cylindrical rock core with black color, length>50 mm, and $RQD>75$	I

101
102
103

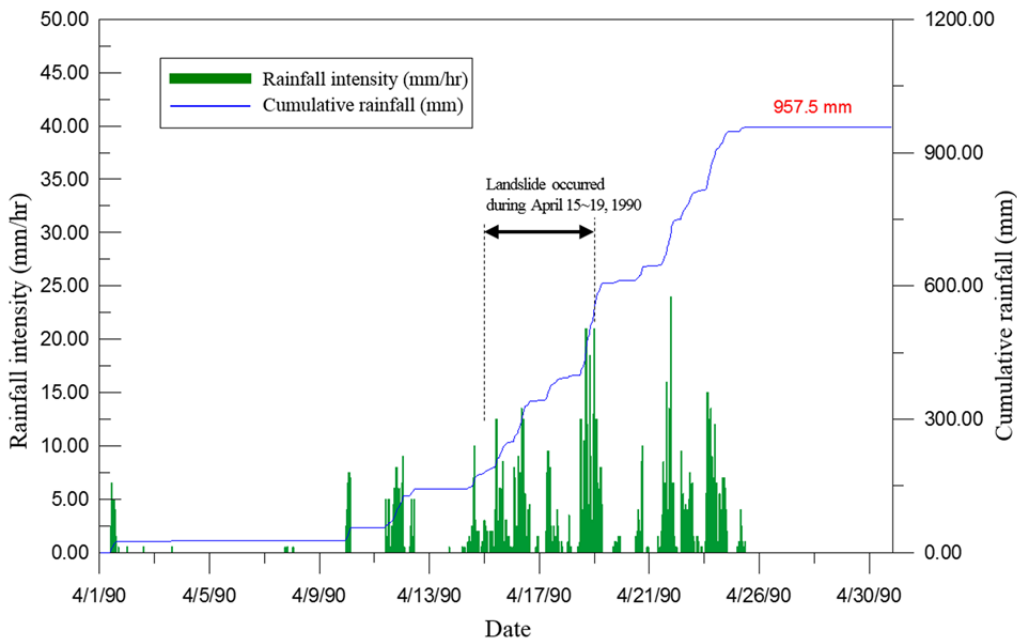
104 **1.3 Landslide in 1990**

105
 106 In 1990 a consecutive torrential rainfall from 11th to 15th, April triggered a massive landslide and damage the Route Tai-7
 107 of central cross-island highway which completely interrupted the transportation of east/west direction. The landslide extends
 108 over a length of 150 m oriented SE to NW with a width of 100 m and a mean slope of 20°. The total volume of the sliding mass
 109 is about $3 \times 10^5 \text{ m}^3$ (or $0.3 \times \text{million m}^3$) with an average thickness of 20 m. As presented in Fig. 4, the catastrophic landslide event
 110 causes a severe depression on the sightseeing industry of Li-Shan and the Li-Shan Hotel was also closed down due to the
 111 detrimental subsidence induced from the landslide. It is generally concluded that the landslide is predominantly caused by the
 112 infiltrated rainwater and poor drainage condition.
 113



114
 115
 116 Fig. 4 Li-Shan landslide on April, 15~19, 1990 (a) sliding mass moves from south to north direction (b) foundation failure of Route Tai-7

117
 118 As illustrated in Fig. 5, a maximum daily rainfall of 155.5 mm occurred on 19th April, 1990 with occurrence frequency of
 119 1.87 years and it is not heavy for a daily rainfall. Nevertheless, the cumulative rainfall for the periods of 10th~20th April, 1990
 120 approximates 586 mm, meanwhile the total cumulative rainfall for the entire April in 1990 can reach 957.5 mm. These records
 121 are maxima with occurrence frequency higher than 50 years when compared with the records of rainfall events in the past. The
 122 infiltrated massive rainwater in the upslope of the sliding body seep downwards and accumulate to raise the groundwater level
 123 and eventually turned into a crucial factor to trigger a large scale landslide. Consequently, the sliding failures of colluviums and
 124 weathered slate in this region (southeast region) can be attributed to the infiltration of rainwater and rise of groundwater level.
 125



126
 127 Fig. 5 Precipitation record of April in 1990 from Li-Shan rainfall monitoring station

128
 129 **1.4 Implementation of Remediation for Li-Shan Landslide**

130
 131 After the large scale landslide in 1990, the field observations showed that the scope and scale of the landslide were
 132 constantly expanding. According to the site investigations on the distribution of sliding bodies within the landslide area from
 133 1990 to 2008, it was found that the scope influenced by sliding bodies and slope failure are exceptionally extensive. The

134 potential sliding surface of Li-Shan landslide is deep-seated approximately at a depth of 30~70 m and spreads in a large area. On
 135 June 25, 1994, a seven years' remediation plan from 1995 to 2002 with total expenditure about 0.915 billion NT\$ was officially
 136 approved by Taiwan government which threw all positive factors such as manpower, financial and material resources into the
 137 remediation works to mitigate the spread potential of the landslide. The remediation plan encompassed drainage galleries,
 138 drainage wells (vertical shaft with radial drainage boreholes drilled at multi-elevation inside the shaft), drainage boreholes at
 139 slope toe (subsurface drainage with shallow depth), submerged dam (for erosion control) and check dam (for sediment control),
 140 as shown in Fig. 6, were implemented to improve the stability of Li-Shan landslide. Conclusively, the main remediation works
 141 of emergency for Li-Shan landslide were the subsurface drainage systems which consists of 15 drainage wells installed from
 142 1995 to 2000, and 2 drainage galleries (G1- and G2-gallery) constructed from 1997 to 2002. It was estimated that the factor
 143 safety of sliding bodies could be promoted up to $F_s=1.2$ for a groundwater level approximately drawn down for 8.5 m (SWCB,
 144 2003). However, it was the first time in Taiwan to perform such enormous plan for landslide remediation and might be also rare
 145 in the case history of slope remediation elsewhere.
 146

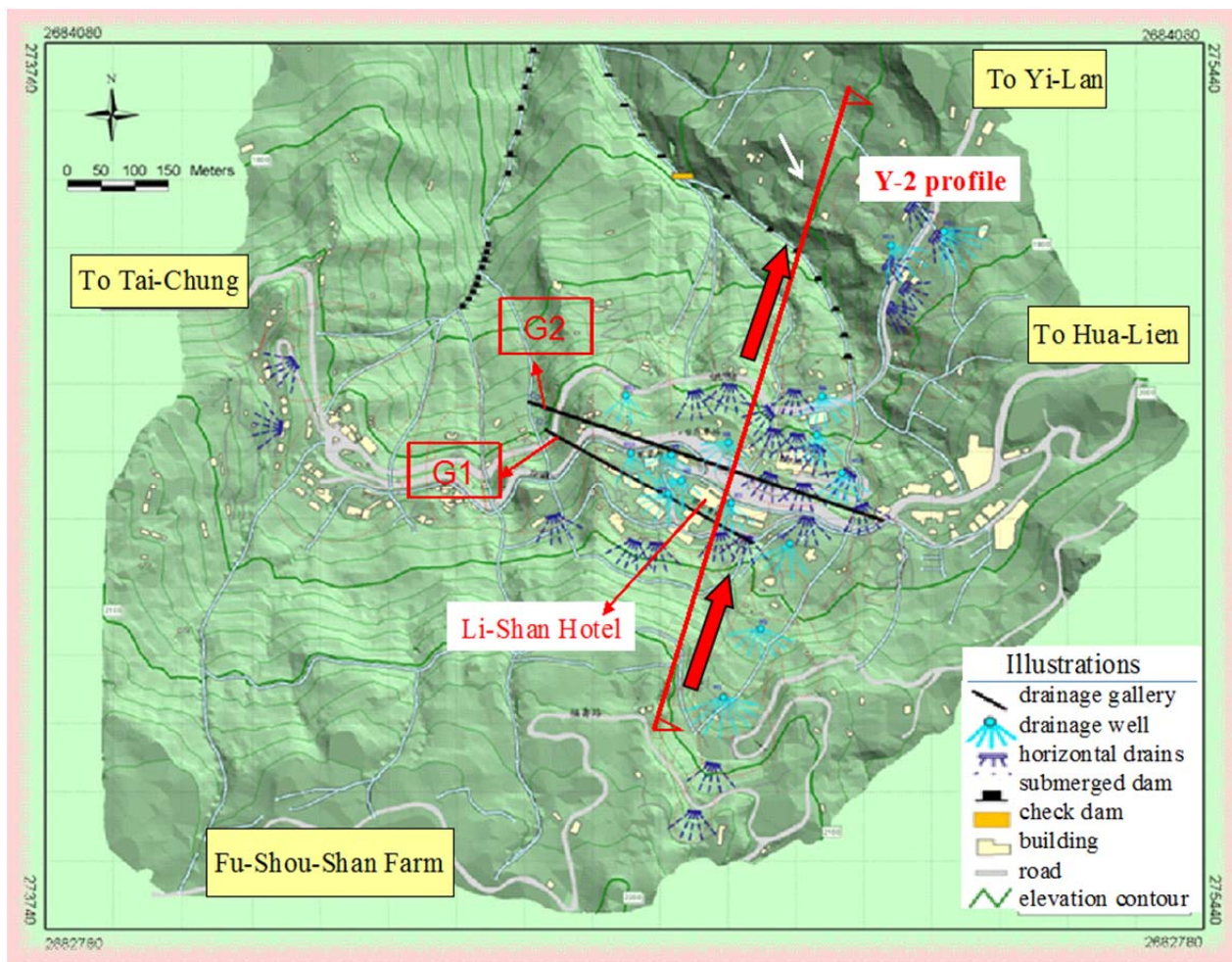


Fig. 6 Configurations of subsurface drainages and remediation works in Li-Shan landslide (SWCB, 2008)

147
 148
 149
 150
 151
 152
 153
 154
 155
 156
 157
 158
 159
 160
 161
 162
 163
 164
 165
 166
 167

2. Subsurface Drainage Systems in Li-Shan Landslides

Li-Shan landslides were frequently triggered by a rise of groundwater level accompanied with increasing pore-water pressure on potential sliding surface. As a result, drainage is by far the most commonly used methods for stabilizing large scale unstable slopes, either alone or in conjunction with other method in Taiwan. Attempts have been made to provide a design method to optimize the number and spacing of horizontal drains (or drainage boreholes) (Kenney et al., 1977; Prellwitz, 1978; Long, 1986). All methods are based on groundwater flow principles and the major difficulty with theoretical design methods is that the permeability is assumed to be constant throughout the ground. Xanthakos et al. (1994) indicated that natural slopes are rarely homogeneous enough to allow reliable subsurface drainage design according to simple principles of dewatering. In addition, Hausmann (1992) suggested that for a successful dewatering system, the designer must have a good understanding of geological structures and choose a drainage system layout that increases the probability of intersecting the major water-bearing stratum. The effectiveness of horizontal drainage system was investigated by Rahardjo et al. (2002, 2003) through a series of numerical analyses on the location and length of horizontal drains (or drainage boreholes). It was found that the horizontal drain is effective in lowering the groundwater table and most effective when located at the bottom zone of a slope. Conclusively, for the design of subsurface drainage systems in Li-Shan landslide, the installation locations of drainage wells and drainage galleries accompanied with well-configured drainage boreholes (or horizontal drains) become extremely crucial to the efficiency of subsurface drainage systems.

168
169
170
171
172
173
174
175

2.1 Drainage Well (Vertical Shaft with Drainage Boreholes)

The drainage well in Li-Shan landslides is a very effective working method to remove the confined groundwater in soil strata and the method was mainly adopted to get rid of the groundwater situating at large depth as illustrated in Fig. 7(a). Large amounts of water can be drained from the slope through drainage wells accompanied with a consequent drop of groundwater levels. Up to the present, there totally 15 drainage wells (1995~2000) were installed in Li-Shan landslides as shown in Fig. 7(b).

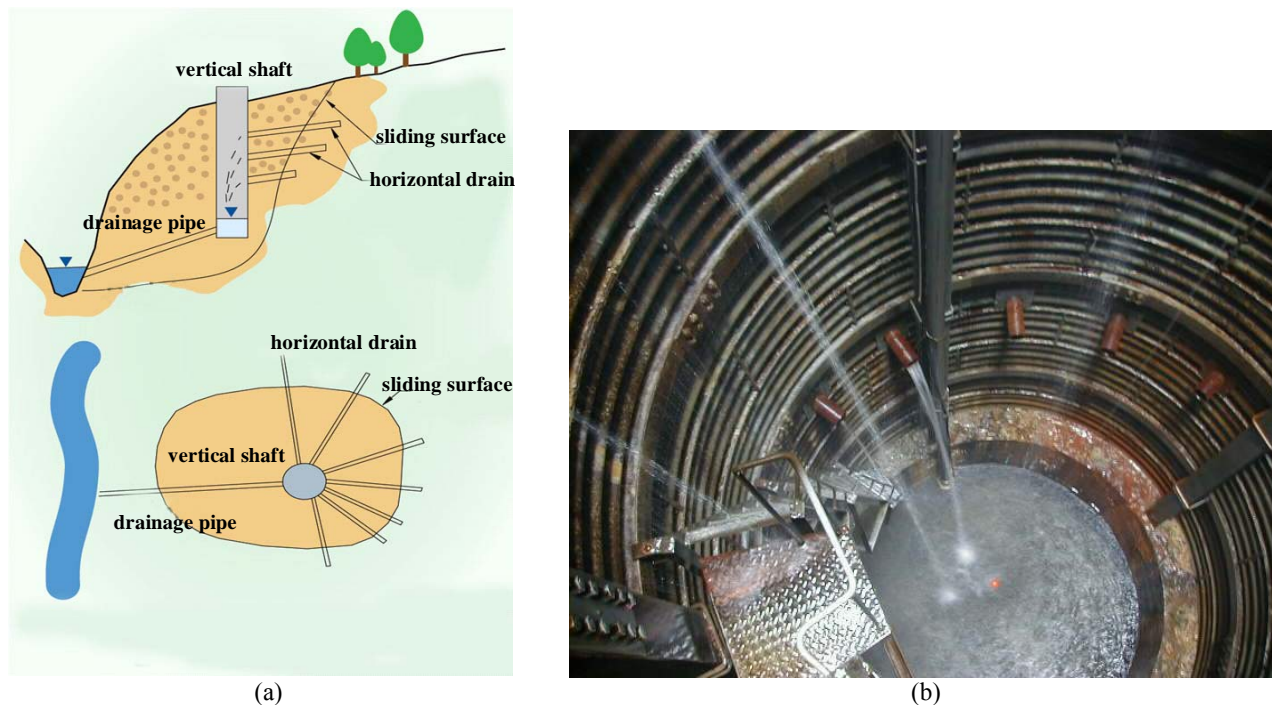


Fig. 7 (a) configuration of vertical shaft with three-level of drainage boreholes (or horizontal drains) in landslide (b) vertical shaft assembled by corrugated steel sheets and collecting groundwater through drainage boreholes (SWCB, 2003)

The vertical shaft was assembled by a continuous galvanized corrugated steel sheet liner with a diameter of 3.5 m and penetration depth of 15~40 m to reach deep-seated potential sliding surfaces. By installing a vertical shaft near the upper portion of sliding body, an array of 5~10 uncased drainage boreholes (spacing about 1.0~2.5 m) with a diameter of 70~100 mm and length of 40~70 m, radiating from the interior of vertical shaft, were drilled at 3 different elevations and inclined 2°~10° (typically 5° to horizontal) upward into the upslope of sliding body. Comparatively, Matti, et. al, (2012) indicated a mean spacing between the drainage boreholes of 10 m is sufficient to control the temporal head fluctuations between the wells within a range of a few meters. In this study, the *Y2-profile* of Li-Shan landslide was adopted for seepage and stability analyses as shown in Fig. 6, and three drainage wells W6, W7 and W8 with a penetration depth of 20, 25, and 15 m respectively were installed adjacent to the *Y2-profile*.

176
177
178
179
180
181
182
183
184
185
186
187
188
189
190
191
192
193
194
195
196

2.2 Drainage Galleries with Sub-vertical Drainage Boreholes

In Li-Shan landslide drainage gallery serves to lower the general groundwater within the landslide mass and to tap into a specific area of high permeability or aquifer at the upper reach of the landslide so that groundwater levels are further reduced. As shown in Fig. 6, at present two drainage galleries totaled about 900 m in length (*G1-gallery*=350 m, 1999~2001; *G2-gallery*=550 m, 1997~2003) passed through the *Y2 profile* at the southeast region of Li-Shan landslide. The gallery portals were located at an elevation of 1,910 m and 1,865 m a.s.l. for *G1-* and *G2-gallery* respectively and the galleries were then excavated from northwest to southeast by an upward grade of 1~2 % to facilitate drainage, as illustrated in Fig. 8. Along the gallery several water-collection chambers with a fan-shaped array of sub-vertical drainage boreholes were drilled to lower the groundwater level under the Li-Shan Hotel. Groundwater is intercepted and evacuated from the potential sliding surface of landslide by gravity through a network of drainage boreholes connected to the water-collection chamber of drainage gallery situated below the potential sliding surface of the landslide. Due to the fact that the depth of potential sliding surfaces of Li-Shan landslide ranges from 30 to 70 m, the drainage galleries were decisively constructed within the intact stable fresh bedrock about 80 m deep underlain the unstable colluviums and weathered bedrock. Eventually the drainage galleries would not influenced by the landslide movements.

As shown in Figs. 9(a) and (b), the gallery has a smaller dimension of 2.07 m×2.1 m (=height×width) with a horseshoe shape cross section and semi-circle crown. Galvanized corrugated steel liner was used for the lateral support of gallery and water-tight concrete drainage ditch was constructed at the base of gallery to drain off the groundwater from the water-collection chambers. As displayed in Figs. 8 and 9(c), 5 water-collection chambers were set up along the *G1-gallery* (10 water-collection chambers along the *G2-gallery*) and each chamber is 6 m long and has an enlarged cross section of 3.0 m×3.0 m (=height×width). Meanwhile, for each chamber there was 18 (=3×6) sub-vertical drainage boreholes (or water collection pipes) with a length of

197 40~60 m were drilled upwards at the crown of gallery to collect and drain off the groundwater from upper soil strata. As shown
 198 in Figs. 8 and 9(a), the average spacing of sub-vertical drainage borehole in a chamber approximates 1.0 m×1.0 m (=transverse
 199 spacing×longitudinal spacing). As a result, there 90 drainage boreholes (=5×18) with a total length of 4,873 m were drilled for
 200 *G1*-gallery (180 drainage boreholes (=10×18) and 10,700 m long for *G2*-gallery). In addition, according to the monitoring data,
 201 the drainage galleries can intercept and drain the groundwater from the sliding bodies by a flow rate Q ranged from 36 to 90
 202 m^3/hr (for *G1*-gallery $Q_{G1}=60\sim90 m^3/hr$, or *G2*-gallery $Q_{G2}=36\sim60 m^3/hr$).
 203

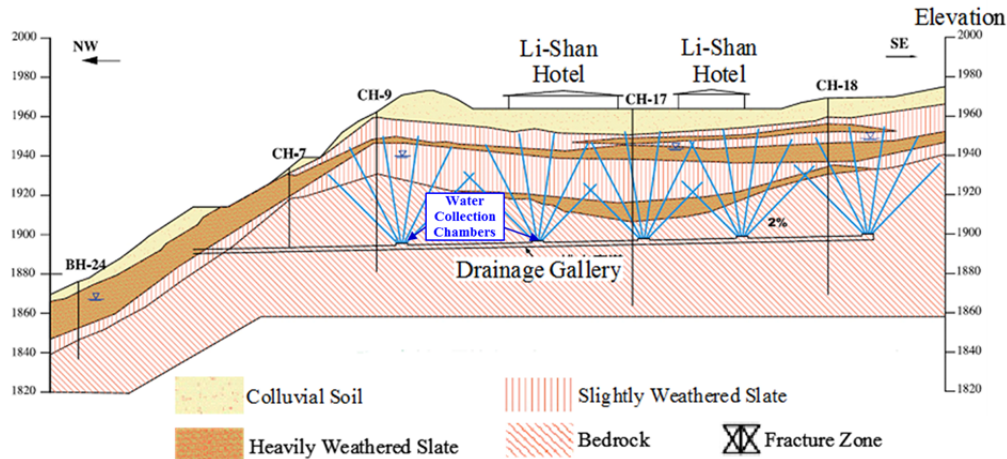


Fig. 8 Geological cross section and location of the drainage gallery (*G1*-gallery)

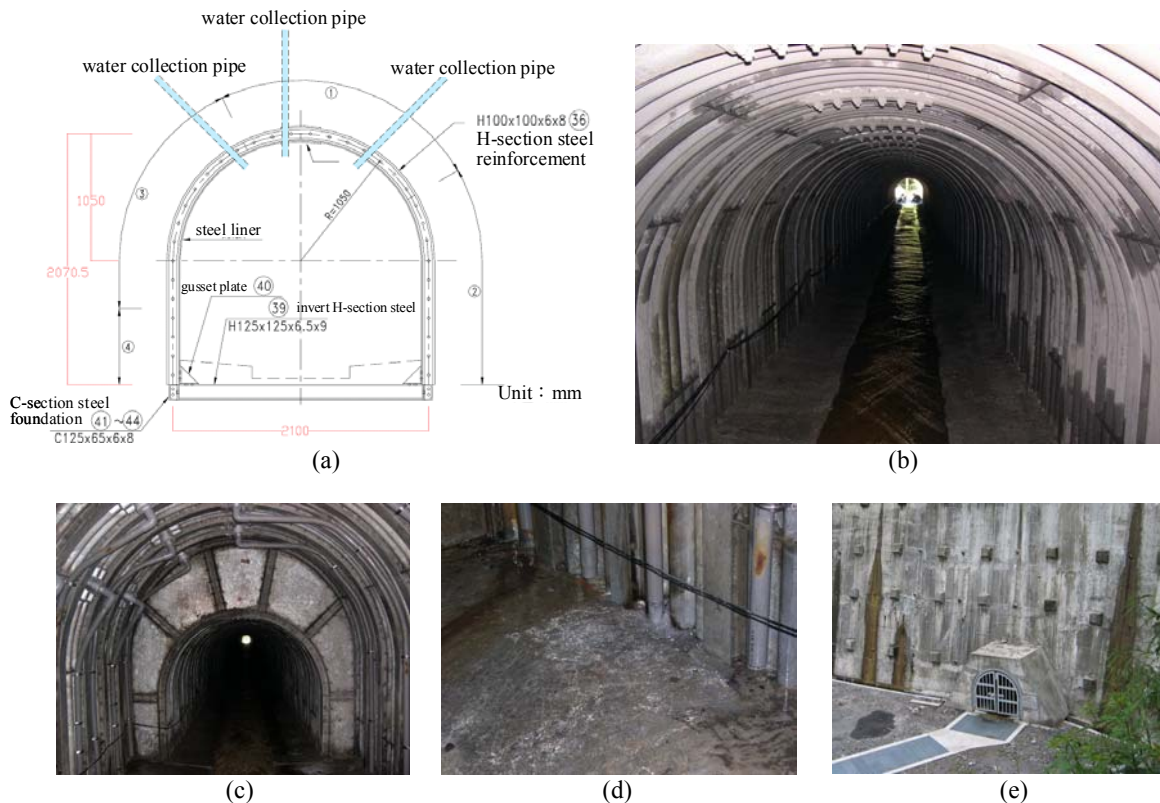


Fig. 9 (a) (b) gallery with a smaller cross sectional layout (width×height=2.07 m×2.1 m) for drainage (c) water-collection chamber with enlarged cross section (width×height=3 m×3 m) and sub-vertical drainage boreholes (water collection pipes) (d) groundwater collected in chamber (e) outlet of gallery

3. Methodology

The *Y2-profile* situates at the southeast region of Li-Shan landslide, as shown in Figs. 6, was selected as a representative profile for numerical analyses. Rainfall-induced seepage analyses and slope stability analyses before and after subsurface drainages remediation were carried out using finite element method (*FEM*) and limit equilibrium method (*LEM*). These two-dimensional (2-D) numerical models evaluate the efficiency of the drainage wells and drainage galleries installed within and below the sliding bodies with the aim of lowering the groundwater levels and promoting the factor of safety of the landslide. Based on the variations of groundwater levels, volumetric water content and factor of safety of the potential sliding bodies, one can recognize the effects of rainfall-induced seepage and subsurface drainages on the slope stability of Li-Shan landslide. The

flow chart of working procedure for the study was illustrated in Fig. 10.

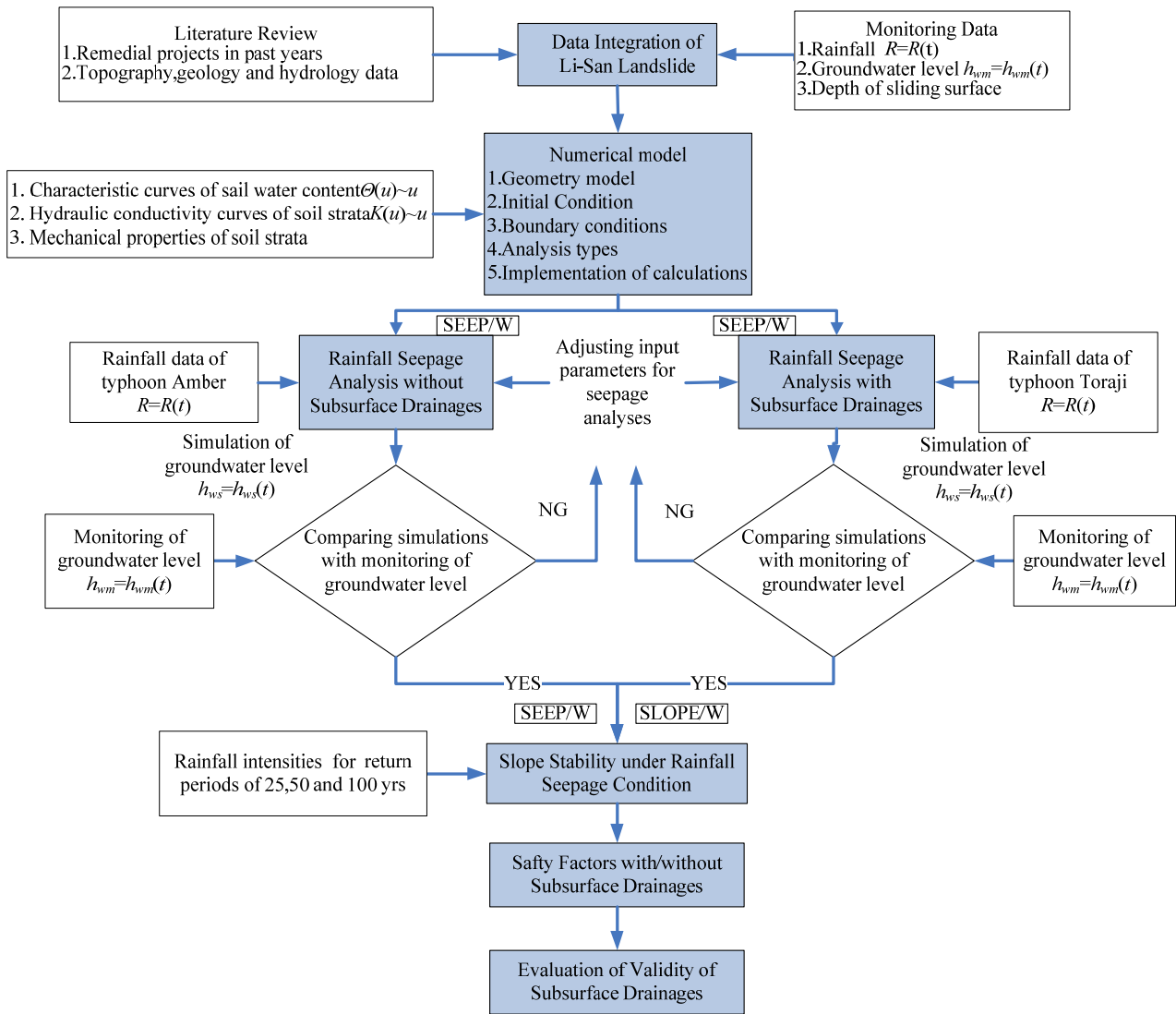


Fig. 10 Evaluation processes for the validity of subsurface drainage systems in Li-Shan landslide

204
205
206
207
208
209
210
211
212
213
214
215
216
217
218
219
220
221
222
223
224
225
226
227
228
229
230

3.1 Initial and Boundary Conditions

The numerical model of geological profile is illustrated in Fig. 11 and a key element in the model is to incorporate the subsurface drainage systems into the simulations. The elevations of left and right boundary of the model are 2,156 and 1,768 m, respectively and the distance of bottom boundary extended from left to right is 830 m. Based on the parametric analyses, Ng, CWW and Shi, Q (1998) evidently indicated that the initial groundwater condition prior to the rainfall has a significant effect on the slope stability. As shown in Fig. 11(a), in numerical model, the *AB* ground surface boundary was specified as a rainfall infiltration boundary, while the *CD* bottom boundary was defined as an impermeable close boundary without seepage (discharge rate $Q=0$). In addition, according to the monitoring data of groundwater levels prior to a rainfall event, the *AD* left boundary and *BC* right boundary were assigned as constant head boundaries with total heads $H= 2,140$ and $1,750$ m respectively. The finite element mesh of numerical model encompassed drainage wells *W-6*, *W-7*, *W-8*, and *H-10*; groundwater level observation wells *B4*, *B5* and drainage galleries *G1*, *G2* located along *Y2-profile* are illustrated in Fig. 11 (b). In addition, it can be found that the subsurface drainage systems were mainly installed at the region of the middle crest or the middle platform of the slope to cope with a large amount of rainwater infiltration during torrential rainfall. This coincides with the numerical results presented by Gasmo J. M. et al. (2000) which reveals that most of infiltration occurs at the crest (or a flat platform) of a slope.

3.2 Numerical Simulation of Subsurface Drainages

The subsurface drainage systems in Li-Shan landslide is comprised of drainage wells and drainage galleries and their drainage effects can be simulated by assigning a series of line-type and point-type drainage boundary conditions along the drainage boreholes in the numerical model.

(1) Drainage wells (Vertical shaft with drainage boreholes)

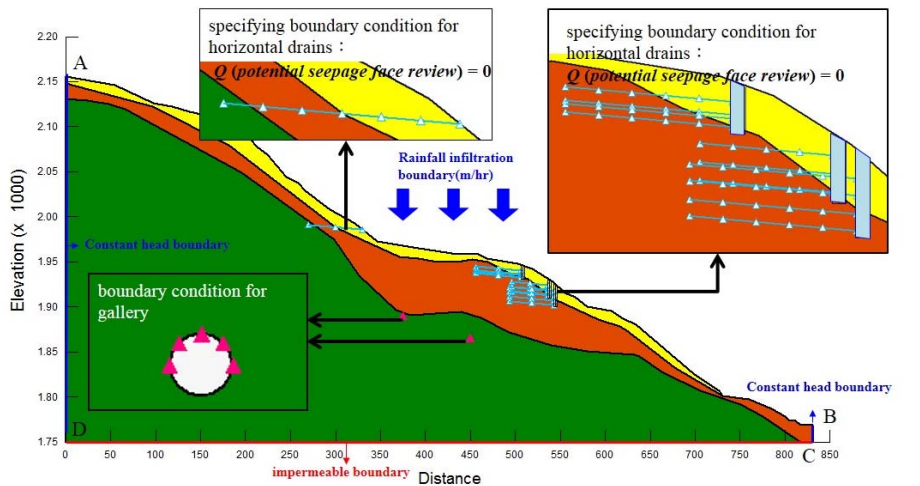
231 The function of drainage boreholes installed at 3~4 different elevations in the vertical shaft (see Fig. 8) can be simulated by
 232 specifying a line-type free seepage surface boundary condition (potential free seepage face review $Q=0$) along the boreholes as
 233 illustrated in Fig. 11. Through this free seepage face, the infiltrated rainwater above the surface was drained out of the
 234 water-bearing layers. Nevertheless, it should be noted that to assign a zero pressure head condition (pressure head $h_p=0$) along
 235 the drainage borehole may lead to some unrealistic numerical results. During the seepage analysis, if a portion of horizontal
 236 drain with zero pressure head boundary condition (pressure head $h_p=0$) situates above the groundwater level at unsaturated zone
 237 (negative pressure head, $h_p<0$) (or the groundwater level is lower than the horizontal drain), eventually the horizontal drain at
 238 unsaturated zone will numerically extract groundwater flow from saturated zone (positive pressure head, $h_p>0$) and this is
 239 unrealistic in engineering practice.

240 **(2) Drainage Galleries with Sub-vertical Drainage Boreholes**

241 An average 5 sub-vertical drainage boreholes with radial array along the crown arch of gallery per unit length of
 242 water-collection chamber (out of plane) are fanning out into the water-bearing stratum to collect groundwater and which can be
 243 simulated by assigning a point-type flow boundary on the 5 installation points of drainage boreholes, as the triangle points
 244 illustrated in Fig. 11(a). In 2-D numerical model, the required input outflow rate of 5 point-type flow boundaries was estimated
 245 according to the measurements of average outflow rate Q_G ($Q_{G1}=60\sim90$ m³/hr, $Q_{G2}=36\sim60$ m³/hr) of the two drainage galleries
 246 $G1$ and $G2$. The drainage rate q_G (m³/hr-m) for each point-type drainage borehole unit length of water-collection chamber (out of
 247 plane) can be estimated as:

248
$$q_G (\text{m}^3 / \text{hr} - \text{m}) = \left(\frac{Q_G}{l_G \times N_G} \right) \div N_C = \left(\frac{Q_G}{L_G} \right) \div N_C$$

249 In which, N_G =number of water-collection chamber along $G1$ - and $G2$ -gallery ($N_{G1}=5$, $N_{G2}=10$); l_G =length of water-collection
 250 chamber along $G1$ - and $G2$ -gallery ($l_{G1}=l_{G2}=6$ m); L_G =total length of water-collection chamber along $G1$ - and $G2$ -gallery= $l_G \times$
 251 N_G ($L_{G1}=6 \times 5=30$ m, $L_{G2}=6 \times 10=60$ m). Moreover, N_C =number of radial drainage boreholes per unit length of water-collection
 252 chamber= $N_{C1}=N_{C2}=5$. Eventually, using the above equation, one can insert 5 nodes ($=N_C$) with an assigned drainage boundary
 253 condition of drainage rate $q_{G1}=0.5$ m³/hr-m and $q_{G2}=0.16$ m³/hr-m to each node for $G1$ - and $G2$ -gallery respectively.
 254



255
256

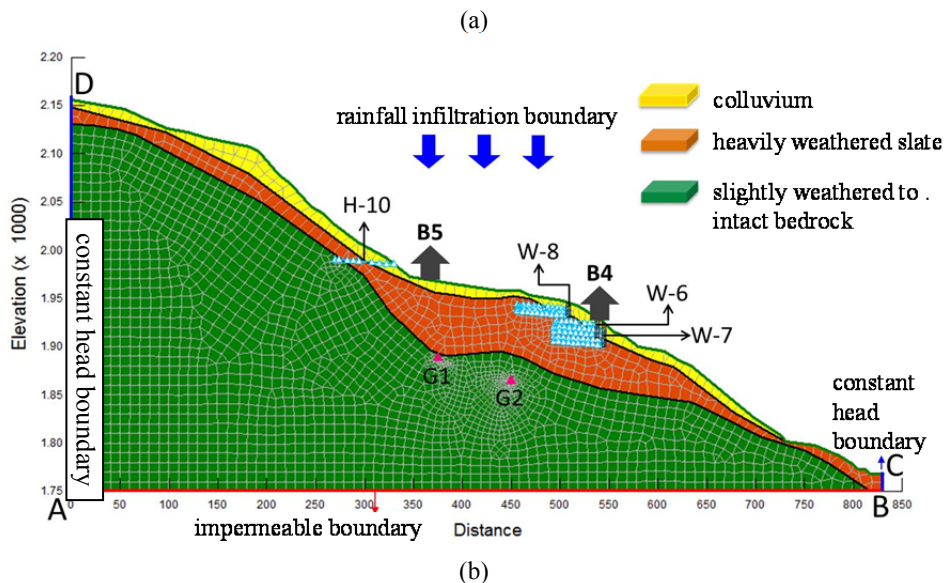


Fig. 11 (a) boundary conditions for subsurface drainages (b) finite element mesh of geological cross section with drainage wells of W-6, W-7, W-8, and H-10; observation wells of B4 and B5 and drainage galleries G1, G2 along Y2-profile

257 **(3) Material Model Parameters.**

258 Prior to the typhoon rainfall event, the slide body above groundwater table comprised of colluviums and heavily to medium
 259 weathered slate is unsaturated, the effects of matric suction on the seepage and stability analyses need to be considered. The soil
 260 water characteristic curve (or SWCC), $\Theta(u_w) \sim u_w$, defines the volumetric water content, $\Theta(u_w)$, corresponding to a specific matric
 261 suction, u_w , (or negative pore-water pressure) and has significant effects on the hydraulic behaviors and shear strength of
 262 unsaturated soil mass. The methods used to determine the SWCC have been studied by many researchers (Green and Corey,
 263 1971; van Genuchten, 1980; Kovács, 1981; Arya and Paris, 1981; Fredlund and Xing, 1994; Aubertin et al., 2001) and most of
 264 the methods are relevant to the grain size distribution curve and physical properties such as porosity and Atterberg's limits of soil
 265 sample. It is common to apply the SWCC to evaluate the hydraulic conductivity curve, $K(u_w) \sim u_w$, required for seepage analysis.
 266 In this study, all the SWCC of soil strata were estimated by their grain size distribution curve. Further, the $K(u_w) \sim u_w$ curve of
 267 soil stratum were determined according to the saturated hydraulic conductivity, K_{sat} , obtained from field pumping test and the
 268 corresponding SWCC proposed by Fredlund and Xing (1994). Tsaparas, et al. (2002) also pointed out that the K_{sat} value has
 269 significant influence on the seepage pattern within an unsaturated soil slope. The required input material model parameters for
 270 rainfall-induced seepage analyses and the sequential slope stability analyses are summarized in Tables 1 and 2. The soil strength
 271 parameters c' and ϕ' were determined directly from direct shear tests and average value of parameters was used for numerical
 272 analyses. Fredlund et al. (1996) developed a simple equation based on the Mohr-Coulomb failure criterion to predict the shear
 273 strength of unsaturated soils. The ϕ^b angle in Table 2 is used to consider the contribution of matric suction to the shear strength
 274 of unsaturated soil and approximates $10^\circ \sim 15^\circ (= \phi^b = \phi'/2)$ for practical purposes
 275
 276

Table 1 Input material model (unsaturated model) parameters for seepage analysis

Soil Type	Saturated volumetric water content Θ_{sat} (%)	Saturated hydraulic conductivity K_{sat} ($\times 10^{-2}$ m/hr)
Colluviums	0.281	5.868
Heavily to medium weathered slate	0.206	2.858
Lightly weathered slate to intact bedrock	0.230	4.9×10^{-4}

$\Theta = S \times n$; $\Theta_{sat} = 1 \times n = n$ (S =degree of saturation, n =porosity)

Table 2 Input material model (Mohr-Coulomb model) parameters for slope stability analysis

Soil Type	Unit volumetric weight γ (kN/m ³)	Cohesion c' (kPa)	Friction angle ϕ' (°)	Equivalent friction angle of matrix suction ϕ^b (°)
Colluviums	17.07	10.79	27	10
Heavily to medium weathered slate	22.56	19.62	28	10
Lightly weathered slate to intact bedrock	27.06	294.3	33	0

(1) γ , c' and ϕ' are determined from field investigations and direct shear tests.
 (2) The modified Mohr-Coulomb failure criterion $\tau = [c' + (\sigma_n - u_a) \times \tan \phi' + (u_a - u_w) \times \tan \phi^b]$ is adopted for slope stability analysis. In which, u_a and u_w represent the pore-air and pore-water pressures of soil mass.
 (3) In the above equation, the ϕ^b angle is used to consider the contribution of matric suction to the shear strength of unsaturated soil.

277
 278
 279

280
 281
 282
 283
 284
 285
 286
 287
 288
 289
 290
 291
 292
 293
 294

3.3 Implementation of Numerical Analyses

Rainfall-induced seepage and slope stability analyses before and after subsurface drainages remediation was performed along *Y2-profile* situated at the southeast region of Li-Shan landslide using Geo-Studio (2012a and 2012b) for the calculations of groundwater levels variation, pore-water pressure distribution, and factor of safety. Rainfall hyetographs of Typhoons Amber (1997) and Toraji (2001), as shown in Figs 12 and 13, were used correspondingly for the analyses without and with remediation. It should be noted that the subsurface drainage systems had not been completed during Amber Typhoon (1997/8/14~1997/8/28) while the meteorological condition with large amounts of precipitation over a relatively short period during Toraji Typhoon (2001/7/29~2001/7/31) was extremely adverse to the slope stability. In addition, Rahardjo (2001) indicated that the antecedent rainfall has significant effects on slope stability. An antecedent rainfall with higher intensity and longer duration enables to preserve water content in soil mass and expedite the infiltration of rainwater from the sequential torrential rainfall which eventually causes slope failure (Sitar, 1992; Tsaparas et al., 2002). As a consequence, the antecedent rainfalls of above two typhoon events were also considered in the rainfall-induced transient seepage analyses of the landslide.

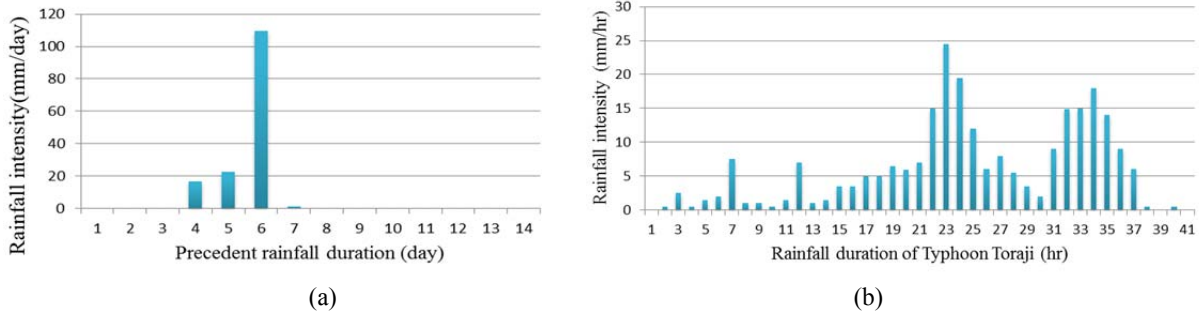


Fig. 12 (a) 14 days antecedent rainfall hyetograph prior to Amber Typhoon (1997/8/14~1997/8/28) (b) rainfall hyetograph of Amber Typhoon (1997/8/28~1997/8/29)

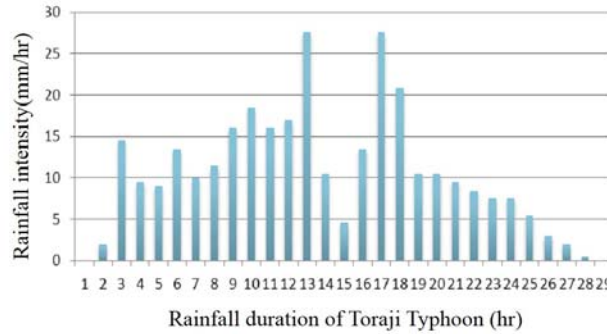


Fig. 13 Rainfall hyetograph of Toraji Typhoon (2001/7/29~2001/7/31)

295
296
297
298
299

4. Results and Discussions

4.1 Verification of Rainfall-Induced Seepage

As shown in Fig. 14, the groundwater level variation of simulation without (Fig. 14(a)) and with (Fig. 14(b)) subsurface drainages remediation is tiny and agree with those of observation from *B5* monitoring station. The slight variation of groundwater level at *B5* monitoring station could be resulted from the geological feature of thin colluviums and thick fractured slate underneath in this area because this makes difficult for the soil strata to accumulate the infiltrated rainwater from long duration rainfall and to raise the groundwater level. In addition, the maximum deviation of the simulation from the observation of *B5* groundwater level without and with subsurface drainage is about 0.5 m and 0.2 m respectively. These deviations are most likely caused by the simplification of 2-D numerical model which unable to capture the effect of 3-D hydrological/geological structure of soil strata.

Conclusively, the proposed numerical procedures can properly simulate the groundwater level variation of *B5* monitoring station with and without subsurface drainages in Li-Shan landslide and the validities of numerical procedures and input model parameters can be verified. The numerical results of seepage analyses enable to provide more realistic and reliable pore-water pressure for the subsequent stability analyses.

4.2 Function of Subsurface Drainages

The objective of the Li-San landslide remediation using subsurface drainage systems aimed at reducing the peak piezometric heads in the slide body by 10~30 m (SWCB, 2003) and facilitate a quick drawdown of rising groundwater level during torrential rainfall. It can be found that the groundwater level (variation at a depth of 50~52 m in Fig. 14(b)) at *B5* monitoring station with subsurface drainages remediation during Toraji Typhoon (2001, peak rainfall intensity=27 mm/hr; rainfall duration $t=29$ hrs) is about 40 m lower than that (variation at a depth of 10~10.5 m in Fig. 14(a)) without remediation during Amber Typhoon (1997, peak rainfall intensity=24 mm/hr; rainfall duration $t=41$ hrs). The large lowering of groundwater levels are mainly caused by the drainage wells (see *H-10*, *W-6*, *W-7*, and *W-8* in Fig. 11(b)) at the central area of the slope which can tap into the colluviums and weathered slate and effectively drain off the infiltrated rainwater in the slope. Meanwhile, to match the calculated groundwater level variations with the observed one, the hydraulic conductivity curve, $K(u_w) \sim u_w$, of various soil strata are made some adjustments and finally determined.

326

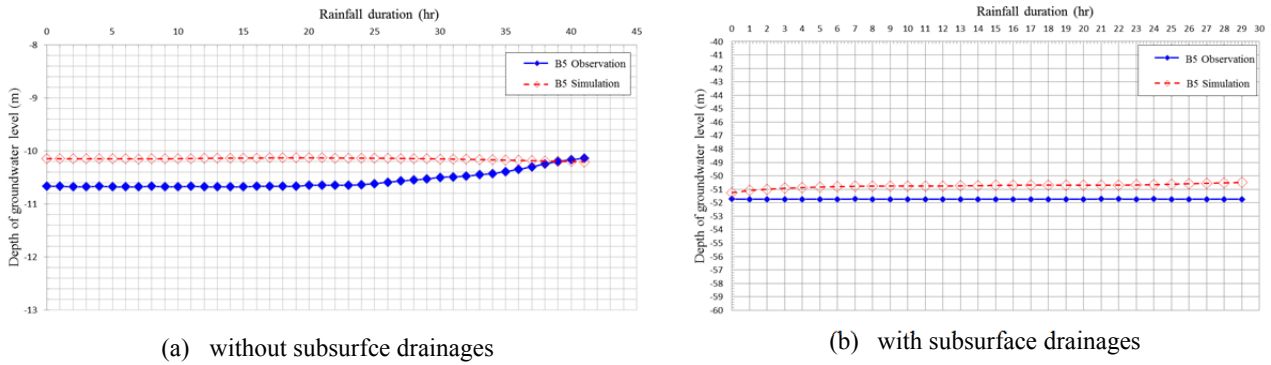


Fig. 14 Comparison of groundwater level variation between simulations and observations at *B5* monitoring station during rainfall of (a) Amber Typhoon (1997), and (b) Toraji Typhoon (2001)

Figure 15 illustrates the effect of the nearby drainage gallery (*GI*-gallery completed in 2001/01) on the long-term (1997/01~2011/11) groundwater levels variation of *B5* monitoring station. The figure gives the elevations of *B5* borehole and groundwater levels before/after construction of *GI*-gallery are 1,968, 1,945, and 1,917 m a.s.l. respectively. It was also indicated that the groundwater levels were lowered down for about 28 m (=1,945 m-1,917 m) during five Typhoon events (Typhoons Mindulle, Haitang, Longwang, Fungwong, and Morakot) after 2001/01.

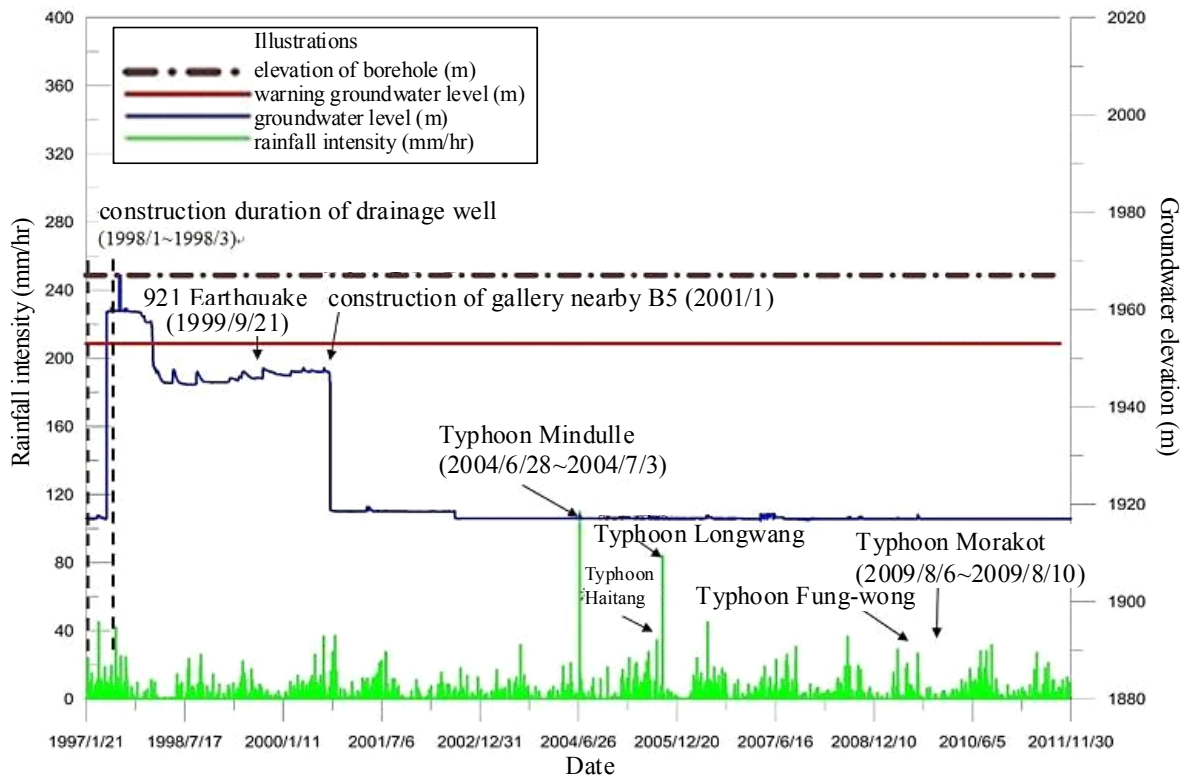


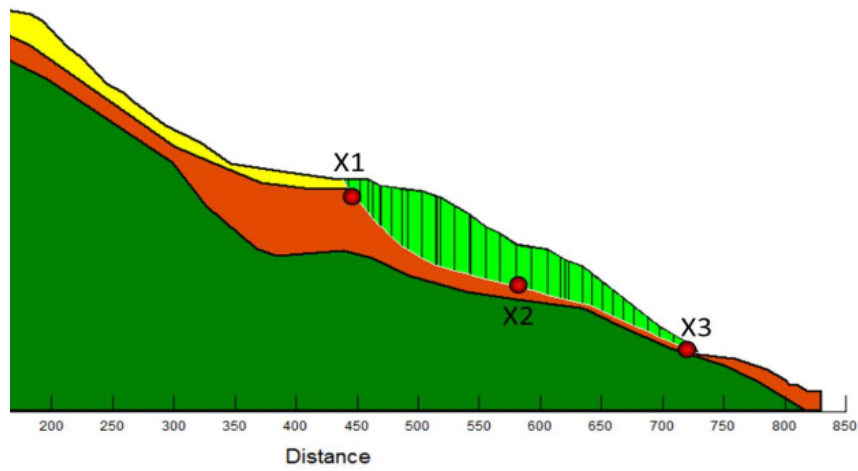
Fig. 15 Groundwater levels variation versus rainfall intensities of *B5* monitoring station (1997/01~2011/11)

4.3 Stability of Potential Sliding Surfaces with and without Remediation

The validity of subsurface drainages in Li-Shan landslide can be evaluated directly from the distribution of pore-water pressure and the corresponding factor of safety, F_s , with and without remediation along Potential Sliding Surface (*PSS*) or indirectly from the distribution of volumetric water content within soil strata during rainfall. In cooperating the inclinometer measurements with stability analyses, three potential sliding surfaces, namely, 1st-*PSS*, 2nd-*PSS* and 3rd-*PSS* as shown in Figs. 16 (a)-(c), can be determined along *Y2*-profile at southeast region of Li-Shan landslide. Their stabilities were diagnosed by inspecting the pore-water pressure of monitoring points (*X1*~*X3* for 1st-*PSS*; *Y1*~*Y3* for 2nd-*PSS*; *Z1*~*Z3* for 3rd-*PSS*) along potential sliding surfaces.

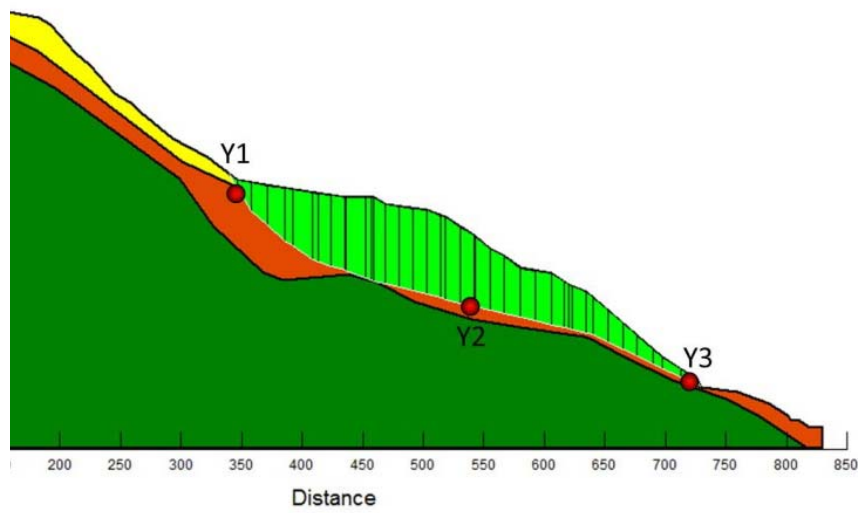
Generally, the F_s value of natural slope in the mountainous area of Taiwan is only slightly greater than unity. Therefore, the slope tends to situate in a marginally stable state ($F_s \approx 1.0$) and is highly sensitive to heavy rainfall or intensive earthquake. In Taiwan, three F_s values are adopted as technical criteria for slope engineering design: (1) for ordinary time $F_s \geq 1.50$, (2) for earthquake $F_s \geq 1.2$, (3) for torrential rainfall $F_s \geq 1.10$. Popescu (2001) proposed a three-stage continuous spectrum of F_s to define the stability state of slopes: $F_s > 1.3$ (stable), $1.0 < F_s < 1.3$ (marginally stable), and $F_s < 1.0$ (actively unstable). The factors of safety, F_s , of the three potential sliding surfaces with and without subsurface drainages were summarized in Table 3. As listed

352 in the table, a higher F_s value with lower decreasing percentage during rainfall is always obtained for the case with subsurface
353 drainages remediation (Toraji Typhoon, 2001) rather than the case without remediation (Amber Typhoon, 1997).



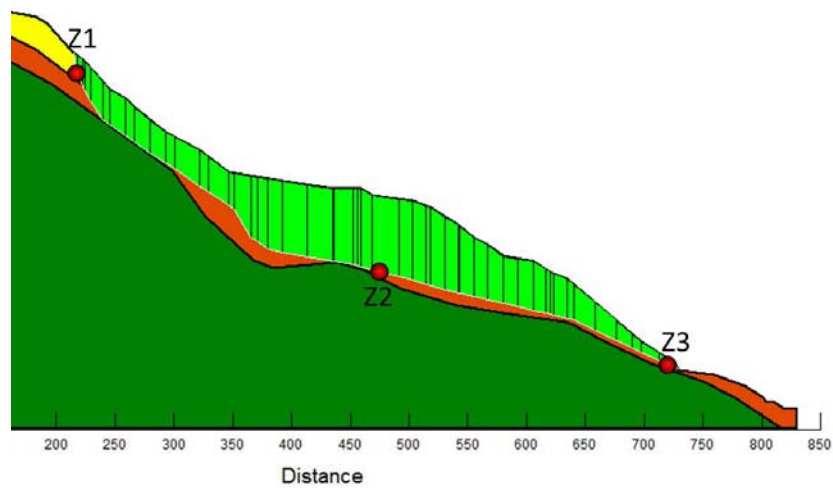
354
355
356

(a)



357
358

(b)



359
360
361
362
363
364
365
366
367
368
369

(c)

Fig. 16 three Potential Sliding Surfaces (PSS) along Y2-profile in Li-Shan landslide and their corresponding monitoring points (a) X1~X3 for 1st-PSS (b) Y1~Y3 for 2nd-PSS (c) Z1~Z3 for 3rd-PSS

Table 3 Factors of safety with and without subsurface drainages along potential sliding surfaces

Potential Sliding Surface (PSS)	Factor of Safety F_s			
	⁽¹⁾ without remediation		⁽²⁾ with remediation	
	Variation during rainfall	Decreasing percentage (%)	Variation during rainfall	Decreasing percentage (%)
1^{st} -Potential Sliding Surface (1^{st} -PSS)	1.148→1.096	4.53	1.240→1.228	0.96
2^{nd} -Potential Sliding Surface (2^{nd} -PSS)	1.317→1.263	4.10	1.521→1.512	0.59
3^{rd} -Potential Sliding Surface (3^{rd} -PSS)	1.250→1.210	3.20	1.459→1.452	0.48

⁽¹⁾Amber Typhoon in 1997 without remediation (Fig. 12) (rainfall duration $t=41$ hr), the subsurface drainages system has not been completed yet in this duration
⁽²⁾Toraji Typhoon in 2001 with remediation (Fig. 13) (rainfall duration $t=29$ hr)
⁽³⁾ $F_s \geq 1.1$ for torrential rainfall; $F_s \geq 1.5$ for ordinary time (stability criteria used in Taiwan)

371

372

(1) Pore-water pressure and Factor of Safety of 1^{st} -PSS during Two Typhoon Events

373

374

375

376

377

According to the numerical results, the F_s value is greatly dependent on the relative locations between the potential sliding surface and the groundwater level. In addition, the groundwater level is dominated by the interaction between rainfall infiltration and subsurface drainage systems. Consequently, a higher factor of safety with lower decreasing rate during torrential rainfall for a potential sliding surface is mainly attributed to the lower down of groundwater level and decrease of pore-water pressure caused by subsurface drainage systems.

378

379

380

381

382

383

Due to the similarity of numerical results for the three potential sliding surfaces, only the factor of safety of 1^{st} -PSS (1^{st} -Potential Sliding Surface, see Fig. 16(a)) F_s with minimum value of 1.096 (see Table 3) and the corresponding pore-water pressure of monitoring points $X1$, $X2$ and $X3$ were presented and discussed in detail. Two typhoon events, Amber Typhoon (1997/8/28~1997/8/29; with 14-days antecedent rainfall: 1997/8/14~1997/8/28) and Toraji Typhoon (2001/7/29~2001/7/31) occurred at different durations were used for the numerical analyses of $Y2$ -profile in Li-Shan landslide without and with subsurface drainages remediation.

384

385

386

387

388

389

390

391

Comparing Fig. 11(b) with Fig. 16(a), it can be seen that the monitoring point $X2$ of 1^{st} -PSS is immediately underneath the drainage boreholes of vertical shafts $W-6$, $W-7$ and $W-8$ and in the vicinity of $G2$ -gallery. In addition, the monitoring point $X1$ also situates at the down slope of drainage boreholes of vertical shaft $H-10$. These indicate the subsurface drainage systems have crucial influence on the seepage behaviours of monitoring points $X1$ and $X2$ during rainfall. Further, because of situating at a lower elevation of slope toe, it is rational to evaluate the efficiency of subsurface drainages by inspecting the response of pore-water pressure of monitoring point $X3$ where tends to accumulate the groundwater flows from upslope. The pore-water pressure distribution of monitoring points $X1$ ~ $X3$ along 1^{st} -PSS is significantly dependent on the variation of groundwater level calculated by the rainfall induced seepage analyses.

392

393

394

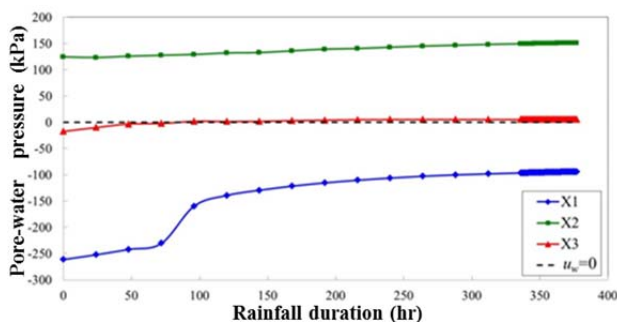
395

396

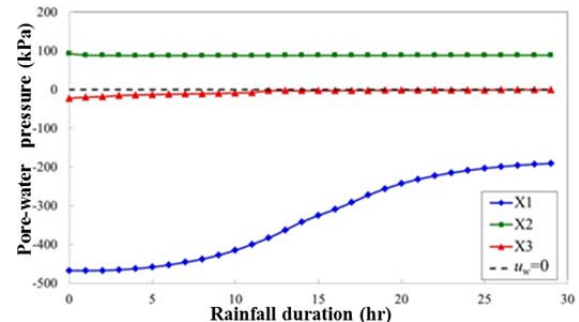
397

398

Before torrential rainfall (rainfall duration $t=0$ hr), for the case without subsurface drainages remediation (Fig. 17(a)), the initial pore-water pressure (u_w) of point $X1$ ($u_w=-261.4$ kPa) and $X3$ ($u_w=-17.4$ kPa) are negative (suction force) due to situating above the groundwater level at unsaturated zone while point $X2$ ($u_w=124.6$ kPa) is positive (squeeze force) below the groundwater level. Comparing with the case with remediation (Fig. 17(b)), the initial pore-water pressure of points $X1$ ~ $X3$ are constantly smaller than that without remediation (Fig. 17(a)) no matter the pressure is negative for points $X1$ ($u_w=-467.5$ kPa) and $X3$ ($u_w=-22.3$ kPa) or positive for point $X2$ ($u_w=92.8$ kPa). This is attributed to the function of subsurface drainages in the ordinary time of non-typhoon seasons.



(a)



(b)

Fig. 17 Variation of pore-water pressure of 1^{st} -PSS (a) Amber Typhoon (1997) without remediation (b) Toraji Typhoon (2001) with remediation

399

400

401

402

403

404

405

During Amber Typhoon in 1997 (rainfall duration $t > 0$ hr), the subsurface drainages remediation has not functioned yet (Fig. 17(a)), the negative pore-water pressure (or suction pressure) of point $X1$ greatly decreases during rainfall ($u_w=-261.4$ kPa→ -94.1 kPa) and the shear strength of soil mass might alternately reduce because of soil matric suction loss. On the other hand, during Toraji Typhoon in 2001 (rainfall duration $t > 0$ hr), due to the function of subsurface drainages (Fig. 17(b)), although the suction loss ($u_w=-467.5$ kPa→ -190.3 kPa) of point $X1$ remains, the final suction pressure is still higher than that during Amber Typhoon ($u_w=-190.3$ kPa $>$ $u_w=-94.1$ kPa). This demonstrates the subsurface drainages enable to mitigate the softening and deterioration of wetting soil mass during torrential rainfall and to prevent a rapid reduction of slope stability.

406 As shown in Fig. 17 (b), the positive pore-water pressure (or squeezing pressure) of point X2 at the middle point of I^{st} -PSS
 407 (see Fig. 16(a)) with subsurface drainages remediation is lower than that without remediation (Figs. 17(a)) and situates in a
 408 stable state throughout the entire rainfall duration under the function of subsurface drainages during Toraji Typhoon.
 409 Additionally, comparing Fig. 17(a) and (b) for monitoring point X2, the squeezing pressure of point X2 increases gradually with
 410 the rainfall duration ($u_w=124.6$ kPa \rightarrow 151.4 kPa) during Amber Typhoon in 1997 (Fig. 17(a)). On the contrary, the squeezing
 411 pressure of point X2 only appears slightly influenced by the infiltrated rainwater during Toraji Typhoon in 2001 (Fig. 17b))
 412 ($u_w=92.8$ kPa \rightarrow 88.5 kPa) and eventually tends a steady condition. This implies the subsurface drainages can suppress an
 413 increase of positive pore-water pressure and situate the slopes in a comparatively stable condition. According to the numerical
 414 results, the stability of I^{st} -PSS is influenced by deeper groundwater flow which cause pore-water pressure increasing on
 415 potential sliding surface rather than by direct infiltration of ground surface. Similarly, Ng, CWW and Shi, Q (1998) pointed out
 416 that rainfall leads to an increase in pore water pressure or a reduction in soil matric suction and in turn, results in a decrease in
 417 shear strength on the potential sliding surface.

418 As shown in Figs. 17(a) and (b), the groundwater flow eventually tends to accumulate at the monitoring point X3, due to
 419 the point situating at a lower elevation of I^{st} -PSS with very thin colluviums overburden (see Fig. 16(a)), the minor suction of
 420 point X3 decreases gradually into a lower level of nearly zero value ($u_w=-17.4$ kPa \rightarrow 0 kPa, for Amber in 1997; $u_w=-22.3$ kPa \rightarrow 0
 421 kPa, for Toraji in 2001) during the rainfalls of the two typhoons. The subsurface drainages remediation has little effect on the
 422 point X3 where is in vicinity of the outlet of the potential sliding surface.

423 In conclusion, the cumulative groundwater in the heavily to medium weathered slate above the I^{st} -PSS and the rainwater
 424 perched between the colluviums and heavily to medium weathered slate was drained out of the sliding mass through drainage
 425 galleries G1 and G2 in a short period. It should be noted that the drainage galleries always situate at the intact fresh slate and
 426 underneath the potential sliding surface (see Fig. 11(b)). Finally, the pore-water pressure distributions in Fig. 17 were then used
 427 to calculate the corresponding factor of safety F_s values of I^{st} -PSS during typhoons, as shown in Fig. 18. For the case without
 428 subsurface drainages remediation (Fig. 18(a)), the F_s values are descending with elapsed time to a minimum value of 1.096
 429 ($=F_{Smin}$) during Amber Typhoon. Comparatively, for the case with remediation (Fig. 18(b)), the F_s values are constantly higher
 430 than those of without remediation and come to a minimum value of 1.228 ($=F_{Smin}$) and almost not affected by Toraji Typhoon.
 431 This demonstrates that the subsurface drainage systems can function effectively to intercept the groundwater flow from
 432 infiltrated rainwater and largely mitigate the rising potential of pore-water pressure on the potential sliding surface which
 433 alternately enables to maintain the slope in a certain stability level during rainfall.

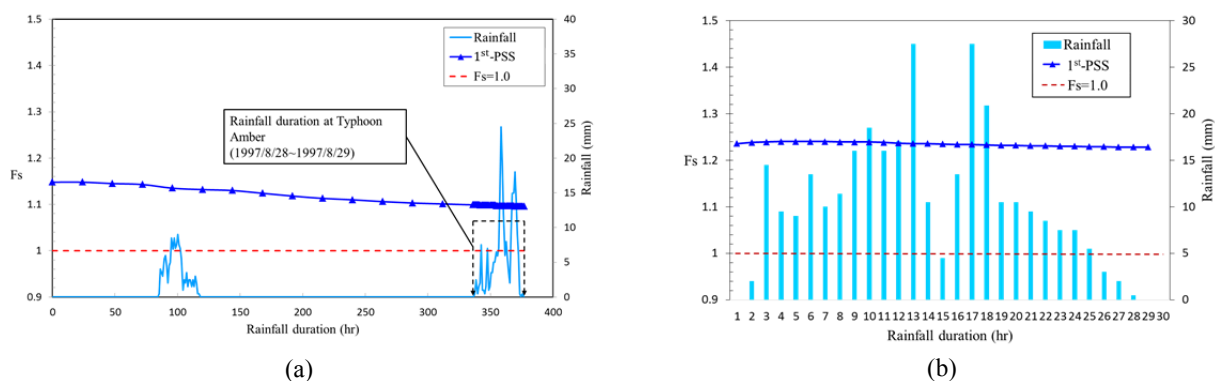


Fig. 18 Variation of factor of safety of I^{st} -PSS (a) Amber Typhoon (1997/8/28~1997/8/29) without remediation (b) for Toraji Typhoon (2001/7/29~2001/7/31) with remediation

434

435

(2) Effects of Fictitious Subsurface Drainages on the Slope Stability of 2^{nd} -PSS during Amber Typhoon

436

437

438

439

440

441

442

443

444

445

446

447

448

449

450

451

452

453

454

455

To understand the effect of subsurface drainages on the slope stability of landslide, a numerical experiments were carried out using Amber Typhoon (1997/8/28~1997/8/29; with 14-days antecedent rainfall: 1997/8/14~1997/8/28; see Fig. 12) for the seepage and slope stability analyses of 2^{nd} -PSS along the Y2-profile of Li-Shan landslide with (fictitious) and without subsurface drainages remediation. Due to the fact that the remediation had not been completed yet during Amber Typhoon in 1997, the drainage wells and drainage galleries were assumed fictitiously to be functional and simulated by assigning specific flow boundary conditions in numerical model. The factors of safety, F_s , of the three potential sliding surfaces with and without subsurface drainages were summarized in Table 4. In addition, Figure 19 shows that during Amber Typhoon the F_s value of 2^{nd} -PSS with subsurface drainages ($F_s=1.403$ at the end of rainfall, for $t=377$ hr) is constantly higher than those without drainages ($F_s=1.263$ at the end of rainfall, for $t=377$ hr) and the potential effect of subsurface drainage systems is evaluated in term of the promotion percentage of F_s value approximates 11.1% ($=[1.403-1.263] \times 100\% / [1.263]$). It should be pointed out that the calculations of F_s value and groundwater level are numerically dependent on the rainfall history (infiltration boundary condition of ground surface) and the subsurface drainage (free seepage surface boundary condition of horizontal drains). In Table 4, the increase of F_s values (at rainfall duration $t=377$ hr) is mainly caused by imposing a fictitious subsurface drainage remediation on the numerical model during Amber Typhoon. As shown in Fig. 19, even though in the time duration without precipitation ($t=120$ hr~340 hr), the fictitious drainage remains functioning and lowering the groundwater level (also increases the F_s value) numerically.

Table 4 Factors of safety without and with fictitious subsurface drainages along potential sliding surfaces during Amber Typhoon in 1997

Potential Sliding Surface (PSS)	Factor of Safety F_S			
	⁽¹⁾ without remediation		⁽²⁾ with fictitious remediation	
	Variation during rainfall	Decreasing percentage (%)	Variation during rainfall	Increasing percentage (%)
1 st -Potential Sliding Surface (1 st -PSS)	1.148→1.096	4.53	1.149→1.201	4.53
2 nd -Potential Sliding Surface (2 nd -PSS)	1.317→1.263	4.10	1.351→1.403	3.85
3 rd -Potential Sliding Surface (3 rd -PSS)	1.250→1.210	3.20	1.304→1.409	8.05

⁽¹⁾Amber Typhoon in 1997 (Fig. 12) (rainfall duration $t=377$ hr) without remediation, the subsurface drainages had not been completed yet in this duration.
⁽²⁾Amber Typhoon in 1997 (Fig. 12) (rainfall duration $t=377$ hr) with remediation, the subsurface drainages was fictitiously assigned in numerical model.
⁽³⁾ $F_S \geq 1.1$ for torrential rainfall; $F_S \geq 1.5$ for ordinary time (stability criteria used in Taiwan)

457
458
459
460
461
462
463
464
465
466
467
468
469
470

Meanwhile, as shown in Fig. 20, prior to the torrential rainfall, the potential sliding surface was submerged by initial groundwater level. Subsequently at the elapsed time of typhoon rainfall, $t=23$ hr, for the occurrence of peak rainfall intensity, the groundwater level ascends for the case without drainages (Fig. 20(a)) and leads to a lower factor of safety $F_S=1.264$. On the contrary, a groundwater drawdown for the case with subsurface drainages (Fig. 20(b)) and a higher factor of safety $F_S=1.399$ can be achieved. Repeatedly, the increase of F_S is due to the fact that the function of fictitious drainage imposed on the numerical model in the time duration without precipitation ($t=0\sim 23$ hr) as shown in Fig. 19. The promotion percentage of F_S value is about 10.7% for a rainfall duration of $t=23$ hr. These results coincide with the study performed by Rahardjo and Leong (2002) that the horizontal drains (or drainage boreholes) are mainly effective to improve the stability of the slope by lowering the groundwater table. Based on the numerical analyses of a field instrumentation case, Rahardjo et al. (2012) also indicated that the F_S values for the slope without horizontal drains are much lower than those of the slope with horizontal drains. Santoso et al. (2009) investigated the influence of (length/spacing) ratio of horizontal drains on residual soil slope stability and found that the promotion percentage of F_S value approximates 12~15 % for a (length/spacing) ratio ranges from 4~9.

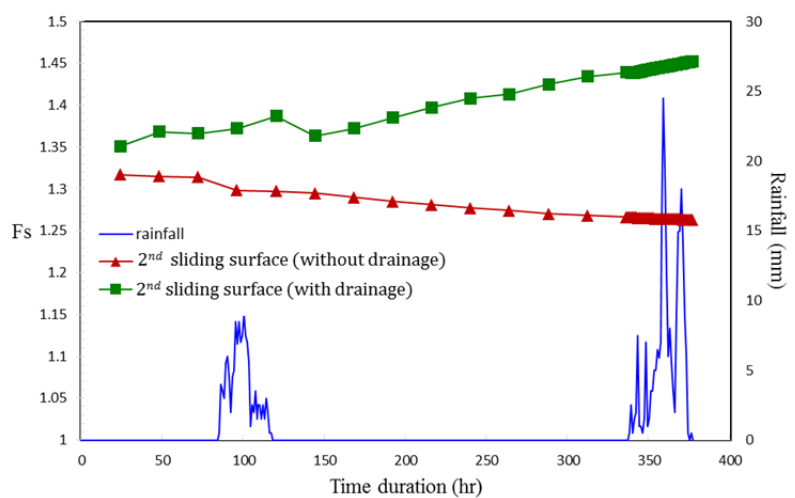


Fig. 19 The factors of safety of 2nd-PSS during Amber Typhoon (1997/8/28~1997/8/29; with 14-days antecedent rainfall during 1997/8/14~1997/8/28)

471
472
473
474

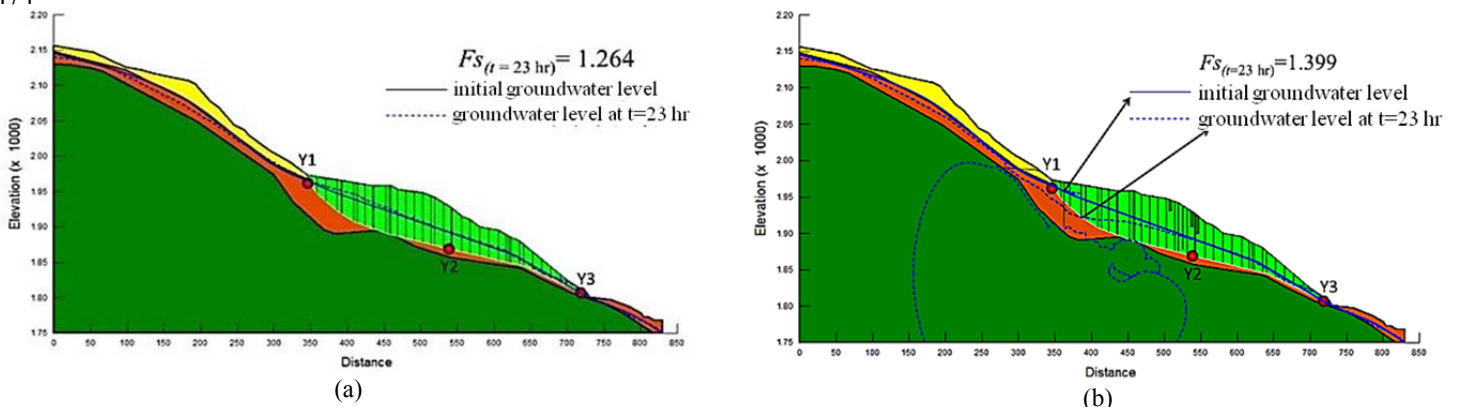


Fig. 20 Groundwater levels and factors of safety of 2nd-PSS at the rainfall duration $t=23$ hr during Amber Typhoon (1997/8/28~1997/8/29) (a) without subsurface drainages (b) with fictitious subsurface drainages

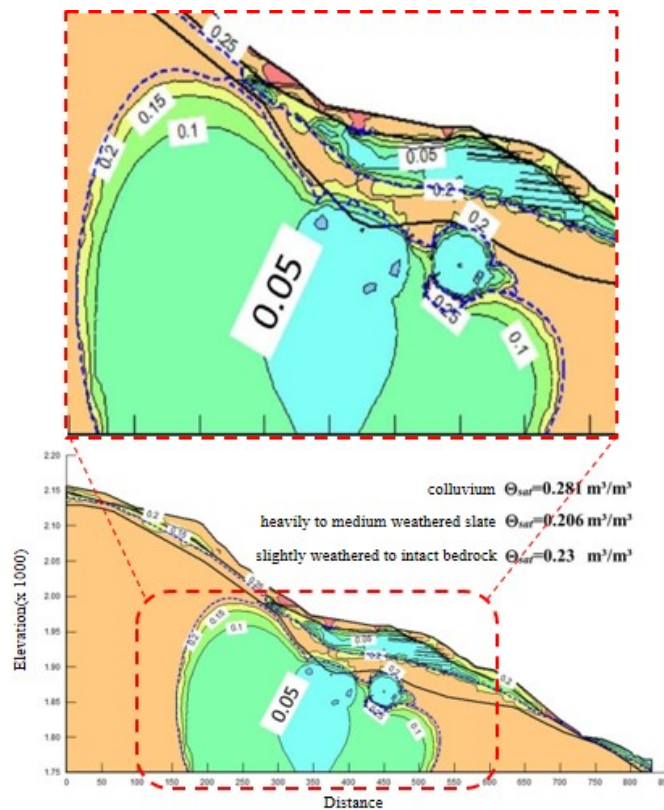
476 Greco et al. (2010) indicated that monitoring of soil volumetric water content seemed more useful than soil suction
 477 monitoring for early warning purposes, since water content grew smoothly during the entire infiltration processes, while soil
 478 suction showed abrupt steep fronts. As illustrated in Fig. 21, the volumetric water contents Θ ($=S \times n=0.05\sim 0.20$, in which, S
 479 $=$ degree of saturation, n =porosity) of colluviums and heavily to medium weathered slate around the drainage galleries $G1$ and
 480 $G2$ during Amber Typhoon are lower than their saturated volumetric water content Θ_{sat} ($\Theta_{sat} =S \times n=1 \times 0.281=0.281$ for
 481 colluviums and $\Theta_{sat}=S \times n=1 \times 0.206=0.206$ for heavily to medium weathered slate). These reveal that in addition to contributions
 482 to groundwater drawdown and pore-water pressure mitigation, the drainage galleries enable to convert the surrounding soil
 483 strata from submerged saturation into unsaturated condition ($\Theta < \Theta_{sat}$) which in turn improve the shear strength of soil mass and
 484 the stability of slope.
 485

486 **(3) Effect of Subsurface Drainage on Volumetric Water Content**

487 Figure 22 illustrates the variation of volumetric water content Θ of soil strata with depth at $B4$ monitoring station without
 488 and with subsurface drainages remediation. For the case without remediation (Fig. 22(a)) during Amber Typhoon
 489 (1997/8/28~1997/8/29), the Θ values are descending gradually to a depth of -30 m under unsaturated condition when comparing
 490 with the saturated volumetric water content Θ_{sat} ($\Theta < \Theta_{sat}$). For colluviums in a depth of 0 ~ -16 m and heavily to medium
 491 weathered slate of -16 ~ -30 m, their Θ_{sat} values are equivalent to 0.281 and 0.206 respectively. On the contrary, for a depth
 492 ranges from -30 to -50 m, the Θ values start to ascend due to approaching the groundwater level which situates at a depth of
 493 around -50 m. Eventually for a depth larger than -50 m, the soil strata are completely submerged and saturated below
 494 groundwater level ($\Theta = \Theta_{sat} = 0.206$).

495 On the other hand, for the case with remediation (Fig. 22(b)) during Toraji Typhoon (2001/7/29~2001/7/31), the
 496 volumetric water content Θ of colluviums near ground surface increases with the rainfall duration from 0.188 ($t=5$ hr) to 0.225
 497 ($t=29$ hr) due to rainwater infiltration and the Θ value for a depth of 0 ~ -10 m resembles to the tendency of the case without
 498 remediation. Subsequently, for a depth of -10 ~ -20 m, although the soil stratum changes from colluvium to heavily to medium
 499 weathered slate at -16 m depth, the Θ values are decreasing with depth constantly from -10 to -20 m to a minimum value of
 500 $\Theta=0.03$. However, the volumetric water content Θ of soil strata adjacent to the ground surface for a depth of 0 ~ -20 m never go
 501 beyond the saturated volumetric water content Θ_{sat} ($\Theta < \Theta_{sat} = 0.281$).

502 It should be noted that $B4$ monitoring station is in the vicinity of drainage wells $W-6$, $W-7$ and $W-8$ (see Fig. 11(b)). At three
 503 different elevation levels from -20 to -40 m along the drainage wells, a series of drainage boreholes were drilled upward into the
 504 upslope of sliding body to collect groundwater, consequently the lower volumetric water content of soil strata within this depth
 505 range is expectable. Similarly, the Θ values start to increase from the depth of -40 to -60 m due to closing groundwater level and
 506 which locates at a depth of around -60 m ($\Theta_{sat}=0.206$) lower than -50 m for the case without drainage remediation (Fig. 22(a)).
 507 This also verifies that the drainage boreholes are of great advantage to the groundwater drawdown during torrential rainfall.
 508



509 Fig. 21 Contour distribution of volumetric water content of soil strata surrounding drainage galleries $G1$ and $G2$
 510
 511

512 **(4) Volumetric Water Content variation with depth during Two Typhoon Events**

513 Figure 22 illustrates the variation of volumetric water content Θ of soil strata with depth at $B4$ monitoring station without
 514 and with subsurface drainages remediation. For the case without remediation (Fig. 22(a)) during Amber Typhoon

515 (1997/8/28~1997/8/29), the Θ values are descending gradually to a depth of -30 m under unsaturated condition when comparing
 516 with the saturated volumetric water content Θ_{sat} ($\Theta < \Theta_{sat}$). For colluviums in a depth of 0~-16 m and heavily to medium
 517 weathered slate of -16~-30 m, their Θ_{sat} values are equivalent to 0.281 and 0.206 respectively. On the contrary, for a depth ranges
 518 from -30 to -50 m, the Θ values start to ascend due to approaching the groundwater level which situates at a depth of around -50
 519 m. Eventually for a depth larger than -50 m, the soil strata are completely submerged and saturated below groundwater level
 520 ($\Theta = \Theta_{sat} = 0.206$).

521 On the other hand, for the case with remediation (Fig. 22(b)) during Toraji Typhoon (2001/7/29~2001/7/31), the
 522 volumetric water content Θ of colluviums near ground surface increases with the rainfall duration from 0.188 ($t=5$ hr) to 0.225
 523 ($t=29$ hr) due to rainwater infiltration and the Θ value for a depth of 0~-10 m resembles to the tendency of the case without
 524 remediation. Subsequently, for a depth of -10~-20 m, although the soil stratum changes from colluvium to heavily to medium
 525 weathered slate at -16 m depth, the Θ values are decreasing with depth constantly from -10 to -20 m to a minimum value of
 526 $\Theta = 0.03$. However, the volumetric water content Θ of soil strata adjacent to the ground surface for a depth of 0~-20 m never go
 527 beyond the saturated volumetric water content Θ_{sat} ($\Theta < \Theta_{sat} = 0.281$).

528 It should be noted that B4 monitoring station is in the vicinity of drainage wells W-6, W-7 and W-8 (see Fig. 11(b)). At three
 529 different elevation levels from -20 to -40 m along the drainage wells, a series of drainage boreholes were drilled upward into the
 530 upslope of sliding body to collect groundwater, consequently the lower volumetric water content of soil strata within this depth
 531 range is expectable. Similarly, the Θ values start to increase from the depth of -40 to -60 m due to closing groundwater level and
 532 which locates at a depth of around -60 m ($\Theta_{sat} = 0.206$) lower than -50 m for the case without drainage remediation (Fig. 22(a)).
 533 This also verifies that the drainage boreholes are of great advantage to the groundwater drawdown during torrential rainfall.

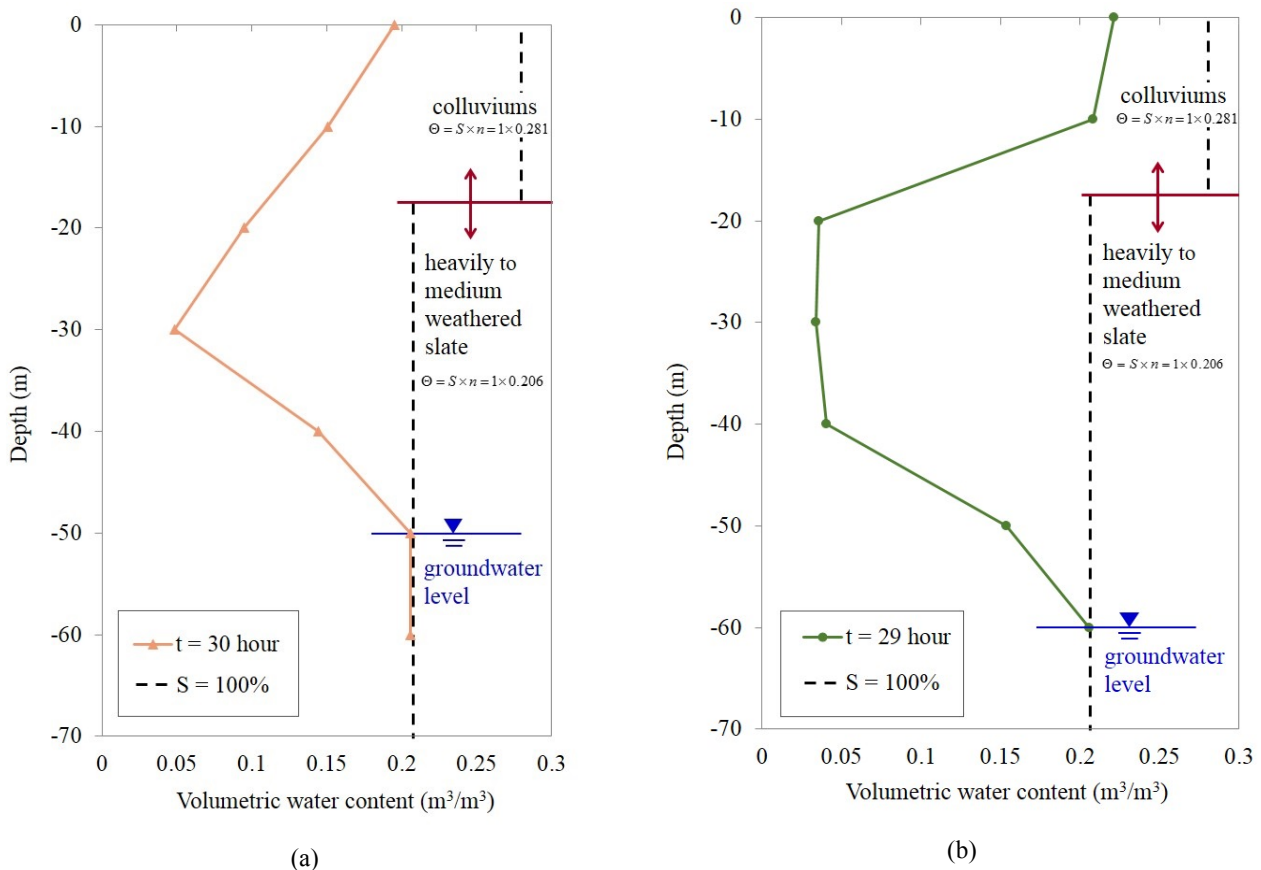


Fig. 22 Variation of volumetric water content with depth at B4 monitoring station (at mid-slope of 2nd-PSS) during
 (a) Amber Typhoon (1997) without remediation (b) Toraji Typhoon (2001) with remediation

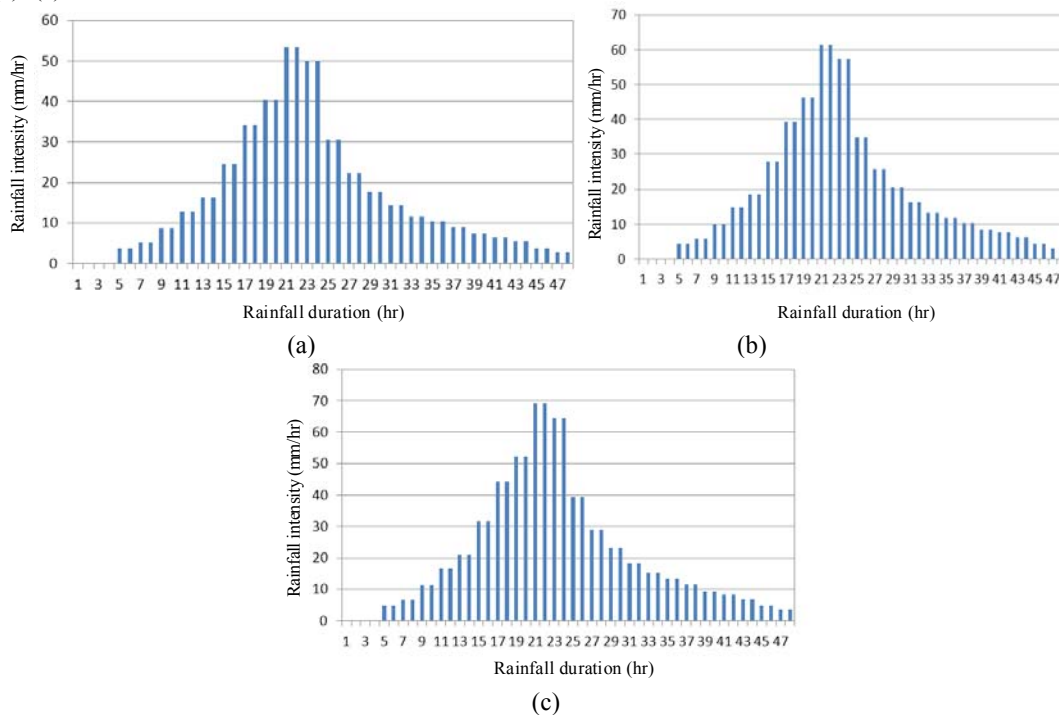
Slope stability analyses have indicated that rainwater infiltration results in a change of suction force and pore-water pressure and the variation of groundwater level is the primary factor affecting the stability of slide mass in Li-Shan landslide. The factor of safety against failure on the three potential sliding surfaces in Y2-profile that passing below the phreatic surface can be improved by subsurface drainages. The increase of unit weight and decrease of shear strength that experienced by the colluviums during torrential rainfall cause the southeast region of Li-Shan landslide particularly susceptible to instability. The subsurface drainages remediation in Li-Shan landslide appears to have been very successful in attaining its objectives and the groundwater levels monitoring data reported have met the requirements of drawdown. Only minor creep movements were measured from field instrumentation in the past years.

534 **(5) Effect of Rainfall Intensity with Different Return Period on Slope Stability**

535 To investigate the effect of rainfall intensity on the stability of Li-Shan landslide and validity of subsurface drainages, three
 536 48-hr design rainfalls with return period of 25, 50 and 100 years for central Taiwan were used for rainfall induced seepage and
 537 stability analyses of the three potential sliding surface in Y2-profile with subsurface drainages remediation. Incorporating the

538
539

rainfall distribution percentage of central Taiwan into rainfall frequency analyses, the design rainfalls can be obtained as shown in Figs. 23(a)~(c).



540
541

Fig. 23 48-hr design rainfall with return period of (a) 25 years (b) 50 years (c) 100 years for central Taiwan

542
543
544
545
546
547
548
549
550
551
552
553
554
555

According to the numerical results, the three design rainfalls with return period of 25, 50 and 100 years have only minor effect on the factors of safety of the three potential sliding surfaces (see Fig. 16) as shown in Table 5. The factors of safety F_S corresponding to the three potential sliding surfaces (1^{st} -PSS, 2^{nd} -PSS and 3^{rd} -PSS) only decrease slightly ($F_S=1.222 \rightarrow 1.220 \rightarrow 1.217$ for 1^{st} -PSS) in response to the three design rainfalls. Meanwhile, the F_S values also constantly maintain higher than unity ($F_S > 1.0$ and $F_S \geq 1.217$) in the entire rainfall duration ($t=48$ hr). As a result, it can be deduced that the capacity of subsurface drainage systems in Li-Shan landslide is sufficient to expedite the drainage of infiltrated rainwater induced from high intensity and long duration rainfall and eventually to maintain the slope stability at a certain standard without further deterioration.

Table 5 Factors of safety of three potential sliding surfaces for 48 hr rainfall duration under design rainfalls with different return periods

Potential Sliding Surface (PSS)	Factor of Safety F_S		
	Return period of 25 years	Return period of 50 years	Return period of 100 years
1^{st} -Potential Sliding Surface (1^{st} -PSS)	1.222	1.220	1.217
2^{nd} -Potential Sliding Surface (2^{nd} -PSS)	1.507	1.505	1.502
3^{rd} -Potential Sliding Surface (3^{rd} -PSS)	1.453	1.452	1.450

$F_S \geq 1.1$ for torrential rainfall; $F_S \geq 1.5$ for ordinary time (Slope stability criteria in Taiwan)

556

5. Conclusions

557
558
559
560
561
562
563
564
565
566
567
568
569
570
571
572

The proposed numerical model is capable of capturing the groundwater responses of sliding body along the $Y2$ -profile at the southeast region of Li-Shan landslide during Amber (1997) and Toraji (2001) Typhoons. In numerical model, the functions of subsurface drainages can be successfully modeled by assigning a line-type free seepage boundary along drainage boreholes for drainage wells and a point-type flow boundary on drainage boreholes for drainage galleries. For Li-Shan landslide, the factors of safety of the three potential sliding surfaces are nearly not influenced by torrential rainfall during Toraji Typhoon after subsurface drainages remediation. Numerically, the subsurface drainages can expedite the drainage of infiltrated rainwater and drawdown of groundwater level to maintain the slope stability at an acceptable standard during torrential rainfall. In addition, the functions of subsurface drainage systems can be verified through the descending volumetric water content of soil strata surrounding the drainage galleries or in a depth from -20 to -40 m of $B4$ monitoring station where three levels of drainage boreholes (or horizontal drains) were drilled for groundwater drainage. In addition, as the return period of design rainfall increasing from 25 years to 100 years, although the factor safety of potential sliding surfaces F_S exhibit a slight decreasing trend for the entire rainfall duration, the F_S values remain constantly greater than unity ($F_S > 1.0$). As a consequence, the subsurface drainage systems of Li-Shan landslide can function well to cope with the infiltration rainwater resulted from torrential rainfall with high intensity and long duration and to prevent the slope from further deterioration. To date, no significant ground movement of the landslide was instrumented after the completion of the subsurface drainage systems. This study makes a

573 contribution to provide a quick computation method and a quantitative indication to evaluate the effectiveness and efficiency of
574 a subsurface drainage system in practice for a large scale landslide.
575

576 **References**

- 577
578
579 Arya, L. M. and Paris J. F. (1981) A physicoempirical model to predict the soil moisture characteristic from particle-size distribution and bulk
580 density data. *Soil Science Society of America Journal*, Vol 45. pp: 1023-1030
581
582 Aubertin, M. Mbonimpa, Bussiere B., and Chapuis R. P. (2001) A model to predict the water retention curve from basic geotechnical properties.
583 *Canadian Geotechnical Journal*, 40(6): 1104-1122 (2003)
584
585 Cai F., Ugai K., Wakai A., Li Q. (1998) Effects of horizontal drains on slope stability under rainfall by three-dimensional finite element analysis.
586 *Computer and Geotechnics* 23, pp 255-275
587
588 Eberhardt E., Bonzanigo L., and Loew S., (2007) Long-term investigation of a deep-seated creeping landslide in crystalline rock. Part II.
589 Mitigation measures and numerical modelling of deep drainage at Campo Vallemaggia. *Canadian Geotechnical Journal*, 44: 1181-1199
590
591 Fredlund, D. G. and Xing, A. (1994) Equations for the Soil-Water Characteristic Curve. *Canadian Geotechnical Journal*, Vol. 31, pp. 521-532
592
593 Fredlund, D. G., Xing, A., Fredlund M. D., and Barbour, S. L. (1996) The Relationship of the Unsaturated Soil Shear Strength to the Soil-water
594 Characteristic Curve. *Canadian Geotechnical Journal*, Vol. 33, pp. 440-448
595
596 Gasmol, J. M., Rahardjo, H. and Leong, E. C. (2000) Infiltration effects on stability of a residual soil slope. *Computer and Geotechnics* 26, pp
597 145-165
598
599 Geo-Studio (2012a) Manual of Seepage Modeling with SEEP/W. Geo-Slope International
600
601 Geo-Studio (2012b) Manual of Stability Modeling with SLOPE/W. Geo-Slope International
602
603 Greco, R., Guida, A., Damiano, E., and Olivares, L. (2010) Soil water content and suction monitoring in model slopes for shallow flowslides
604 early warning applications. *Physics and Chemistry of the Earth*, 35, 127-136
605
606 Green, R. E. and Corey, J. C. (1971) Calculation of Hydraulic Conductivity: A Further Evaluation of Some Predictive Methods. *Soil. Sci. Am.*
607 *Proc.* 35, pp. 3-8
608
609 Hausmann, M. R. (1992) Slope Remediation, Proceedings: Stability and Performance of Slopes and Embankments-II. ASCE, Geotechnical
610 Special Publication No. 31, Berkeley, California, pp. 1274-1317
611
612 Kovács, G. (1981) Seepage Hydraulics. *Developments in Water Science* 10, Elsevier Science
613 Publishers, Amsterdam
614
615 Kenney, T. C., Pazin, M., and Choi, W. S. (1977) Design of Drainage boreholes for Soil Slopes. *Journal of the Geotechnical Engineering*
616 *Division, ASCE*, Vol. 103, GT 11, November, pp. 1311-1323
617
618 Lau, K.C. and Kenney, T.C. (1984) Horizontal drains to stabilize clay slopes. *Canadian Geotechnical Journal*, 21, pp. 241-249
619
620 Long, M. T. (1986) Camp Five Slide—Exploration, Design and Construction of a Horizontal Drain Solution. Proceedings, 22nd Symposium on
621 Engineering Geology and Soils Engineering, Boise, Idaho, pp246–265
622
623 Matti B., Tacher L., and Commend S. (2012) Modelling the efficiency of a drainage gallery work for a large landslide with respect to
624 hydrological heterogeneity. *Canadian Geotechnical Journal*, 49: 968-985
625
626 Nakamura, H. (1988) Landslide control works by horizontal Drainage works. Proceedings 5th International Symposium on Landslides,
627 Lousanne, Vol. 2
628
629 Ng, C. W. W. and Shi, Q. (1998) A Numerical Investigation of the Stability of Unsaturated Soil Slopes Subjected to Transient Seepage.
630 *Computers and Geotechnics*, Vol. 22, No.1, 1-28
631
632 Nonveiller, E. (1981) “Efficiency of horizontal drains on slope stability”. Proc. 10th International Conference on Soil Mechanics and Foundation
633 Engineering, Stockholm, 3, pp. 495-500.
634
635 Popescu, M. E. (2001) A suggested method for reporting landslide remedial measures. *IAEG Bulletin*, 60(1):69-74
636
637 Prellwitz, R. W. (1978) Analysis of Parallel Drains for Highway Cut Slope Stabilization. Proceedings, 16th Annual Engineering Geology and
638 Soils Engineering Symposium, Boise, Idaho, pp. 153-180
639
640 Rahardjo, H., Li, X. W., Toll, D. G. and Leong, E. C. (2001) The effect of antecedent rainfall on slope stability. *Journal of Geotechnical and*
641 *Geological Engineering, Special Issue on “Unsaturated and Collapsible Soils”* pp371-399
642
643 Rahardjo, H., and Leong, E. C. (2002) Horizontal Drains in Unsaturated Soil Slopes. Proc. 3rd International Conference on Unsaturated Soils,
644 Recife, Brazil, pp773-777
645
646 Rahardjo, H., Hritzuk, KJ, Leong, EC, and Rezaur, R. B. (2003) Effectiveness of drainage boreholes for slope stability, *Engineering Geology*,
647 2154, 1-14
648
649 Rahardjo, H., Satyanaga1, A., Leong E. C. (2012) Unsaturated Soil Mechanics for Slope Stabilization, *Geotechnical Engineering Journal of the*
650 *SEAGS & AGSSEA*, Vol. 43, No.1, pp48-58

651
652 Sitar, N., Anderson, S. A., and Johnson, K. A. (1992) Conditions for initiation of rainfall-induced debris flow. Stability and performance of
653 slopes and embankments-II, Volume 1, pp. 843-849, Proceedings of a special conference at U. C. Berkeley, ASCE
654
655 Soil and Water Conservation Bureau, Taiwan (2003) Handbook: A brief description of remedial plan for Li-Shan landslide area
656
657 Soil and Water Conservation Bureau, Taiwan (2008) Handbook: A brief of remedial work for landslide in Li-Shan Area
658
659 Tacher, L., Bonnard, C., Laloui, L., and Parriaux, A. (2005) Modelling the behaviour of a large landslide with respect to hydrogeological and
660 geomechanical parameter heterogeneity, Landslides, 2:3-14
661
662 Tsaparas, I., Rahardjo, H., Toll, D. G., and Leong, E. C. (2002) Controlling parameters for rainfall-induced landslides. Computers and
663 Geotechnics, Vol. 29, No. 1, pp. 1-27
664
665 van Genuchten, M Th. (1980) A closed-form equation for predicting the hydraulic conductivity of unsaturated soils. Soil Science Society of
666 America Journal, Vol. 44, pp: 892-898
667
668 Xanthakos, P. P., Abramson, L. W., and Bruce D. (1994) Ground Control and Improvement. New York: Wiley